NUCLEATE BOILING HEAT TRANSFER

by

LIANG-CHUAN PENG
Diploma, Taipei Institute of Technology, 1960

A MASTER'S REPORT

submitted in partial fulfillment of the

requirements for the degree

MASTER OF SCIENCE

Department of Mechanical Engineering

KANSAS STATE UNIVERSITY
Manhattan, Kansas

1966

Approved by:

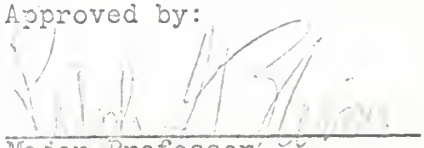

Major Professor

TABLE OF CONTENTS

page

1. INTRODUCTION 1

1-1. Review of Previous Developments. 1

1-2. Purpose and Outline of the Report. 3

1-3. Significance of the Results. 4

2. SOME FUNDAMENTAL FEATURES OF NUCLEATE BOILING HEAT TRANSFER 6

2-1. Regimes of Boiling Heat Transfer 6

2-2. General Consideration of Bubble Dynamics . . . 7

2-3. Factors Affecting Nucleate Boiling Heat Transfer 13

2-4. Some Proposed Mechanisms 18

3. TRIPLE INTERFACE EVAPORATION 26

3-1. Contribution of Bubble Latent Heat 26

3-2. Triple Interface Evaporation 30

3-3. Bubble Growth Rate and Correlation of Heat Flux 36

3-4. Maximum Heat Flux and Factors Affecting Nucleate Boiling Heat Transfer 45

3-5. Conclusion 54

ACKNOWLEDGEMENT. 56

NOMENCLATURE 57

REFERENCES 59

APPENDIX 1 64

APPENDIX 2 67

APPENDIX 3 70

LIST OF ILLUSTRATIONS

Figure		Page
1	Regimes of pool boiling.	6
2	Typical shapes of cavity	9
3	Bubble growth on the wall.	10
4	Effect of heating surface (12)	15
5	Effect of mechanical agitation (2)	16
6	Typical boiling data for subcooled forced convection (2)	17
7	Data of Fig. 6 as a function of Δt_{sat}.	19
8	Effect of pressure (3)	20
9	Stirring effect of bubbles	21
10	Vapor-liquid exchange action	22
11	Temperature of liquid exchanged.	24
12	Microlayer evaporation	25
13	Heat flux through latent heat transport.	26
14	Schematic diagram of power boiler.	29
15	Discontinuity in triple interface.	32
16	General behavior of triple interface discontinuity	35
17	Capillary wicking (49)	36
18	Bubble growth on the wall.	38
19	Variation of detaching diameter with population (51)	42
20	Relation between superheat and bubble population.	43
21	Bubble packaging	46
22	Effect of temperature and pressure	52
23	Factors affecting nucleate boiling heat transfer	53

1. INTRODUCTION

In spite of its familiarity to mankind, boiling liquids have not been given much consideration until very recently. The tremendous study of boiling stems from the development of high heat flux equipment such as nuclear reactors and rocket engines. The heat flux carried by boiling is usually the order of 10^6 BTU per square foot per hour, which is far beyond what a non-boiling liquid can achieve.

1-1. Review of Previous Developments

The general subject of boiling heat transfer is discussed in detail in references (1)-(6)*. The systematic study of boiling began in 1934 when Nukiyama (7) published his first boiling curve. Since then rather wide attention has been received. Prior to 1950, all the studies were limited to pure empirical correlation. Some equations had been published (8-12), but no one of them was successful enough to warrant widespread adoption (4).

In 1951, a semi-theoretical method was adopted, which resulted in the publication of the well-known Rohsenow's equation (13) and the equation of Forster and Zuber (14). Both assumed the major portion of the heat is transferred from the solid to the liquid bulk; the contribution of bubble latent heat was considered negligible. This was based mainly

---

*Numbers in parenthesis refer to references listed at the end of the report.

on the experiments (15-16) observed from subcooled liquids where the visible latent heat carried by bubbles contributed only 1% or 2% of the total heat flux. Heat transfer is considered as turbulent forced convection stirred by bubble growth and detaching velocities. Thus, most of the proposed correlations (13) (14) (17) (18) were of the form

$$N_{Nu} = \text{Const } (N_{Re})^m (N_{Pr})^n$$

where the constant and the exponents m and n are determined from experiments. At a particular pressure and for a given surface-liquid combination, this equation reduces approximately to

$$q/A = \text{Const } (\Delta t_{sat})^a$$

But this form of correlation fails to take care of the nucleate characteristics of the heating surface. Then Yamagata and Nishikawa (19) proposed a revised form. That is:

$$q/A = \text{Const } N^b (\Delta t_{sat})^c$$

The exponents determined by Yamagata and Nishikawa were $b = \frac{1}{4}$, $c = \frac{3}{2}$; by Zuber (20) were $b = \frac{1}{3}$, $c = \frac{5}{3}$; and by Tien (21) were $b = \frac{1}{2}$, $c = 1$. A more detailed discussion of this development was treated by Sato (22) and Zuber (23).

Up to the end of the 1950's, it was concluded that latent heat transport played only a minor role in nucleate boiling. But this conclusion has had considerable modification since

Moor and Mesler (24) have successfully measured the unusual cooling effect of the bubble base. At about the same time, Bankoff (25) carried out another experiment which showed that high heat transfer rates existed at the boundary between the steam bubble and the turbulent subcooled liquid stream. A critical survey of this advancement was also done by Bankoff (26) in 1962. Later a further report of the bubble cooling effect was published by Rogers and Mesler (27). The most recent report about latent heat transport is due to the work of Rallis and Jawurek (28). They showed that latent heat transport $(q/A)_{LH}$ is significant at all stages, the ratio $(q/A)_{LH}/(q/A)_{TOT}$ increases steadily with increasing heat flux and appears to tend to unity as the total heat flux tends toward burnout.

Now the importance of latent heat transport seems rather clear. In general, the total observed heat flux is contributed by microlayer convection together with latent heat transport and the latter becomes dominant as heat flux approaches the burnout point. But to the writer's knowledge, no correlation based on the latent heat transport has yet been attempted.

1-2. Purpose and Outline of the Report

Although it seems clear that latent heat transport in nucleate boiling is significant, further verification is required. The purpose of this report is to substantiate

the heat flux contributed by latent heat transport and to give a theoretical analysis of this mechanism.

In Section 2, some fundamental features of boiling heat transfer are summarized which will be helpful in the development of the main part of this report.

In Section 3, typical data of saturated boiling heat transfer are analyzed first to show the numerical fraction of the visible latent heat contributed in saturated liquid boiling. Then the path of the heat flow passing through the bubble is studied. A triple interface evaporation mechanism is thus proposed. Finally, the peak flux and the affecting factors are discussed.

1-3. Significance of the Results

A brief calculation from the data of Westwater and Santangelo (29) showed that the visible bubble latent heat carried by a detaching bubble is about 50% of the total heat flux observed. Careful examination reveals that the heat flux passes through the bubble via a very slim area near the solid-liquid-vapor triple interface (or line). The triple interface evaporation mechanism proposed is based on this investigation. Following this mechanism, bubble growth rate is given as

$$r = \text{Const } (\theta \tan \frac{B}{2})^{\frac{1}{2}}$$

which agrees with the recent experiment observed by Johnson

and others (30). An analytically derived correlation equation has the form

$$q/A = \text{Const } Nd_o \frac{L^2}{RT_{sat}^2} \exp\left(-\frac{L}{RT_{sat}}\right)\Delta t_{sat}$$

where the constant, according to kinetic theory of gas and liquid, should depend on the type of liquid. An explanation of the affecting factors using this equation has worked very well.

Since the correlation made in this report is due to the part of heat flux contributed by latent heat transport only, it can be considered correct only at the high heat flux range where convective heat transfer is negligible. However, the equation for bubble growth rate is always correct.

2. SOME FUNDAMENTAL FEATURES OF NUCLEATE BOILING HEAT TRANSFER

2-1. Regimes of Boiling Heat Transfer

The systematic study of boiling heat transfer began with the discovery of the unstable region by Nukiyama (7) in 1934. While boiling a pool of water with an electrically heated wire, Nukiyama found several regimes existing as the temperature driving force increased gradually. Fig. 1 shows these typical regimes in pool boiling. In region AB, though the wall temperature is higher than the saturation temperature, no boiling occurs at the heating surface. Water evaporates

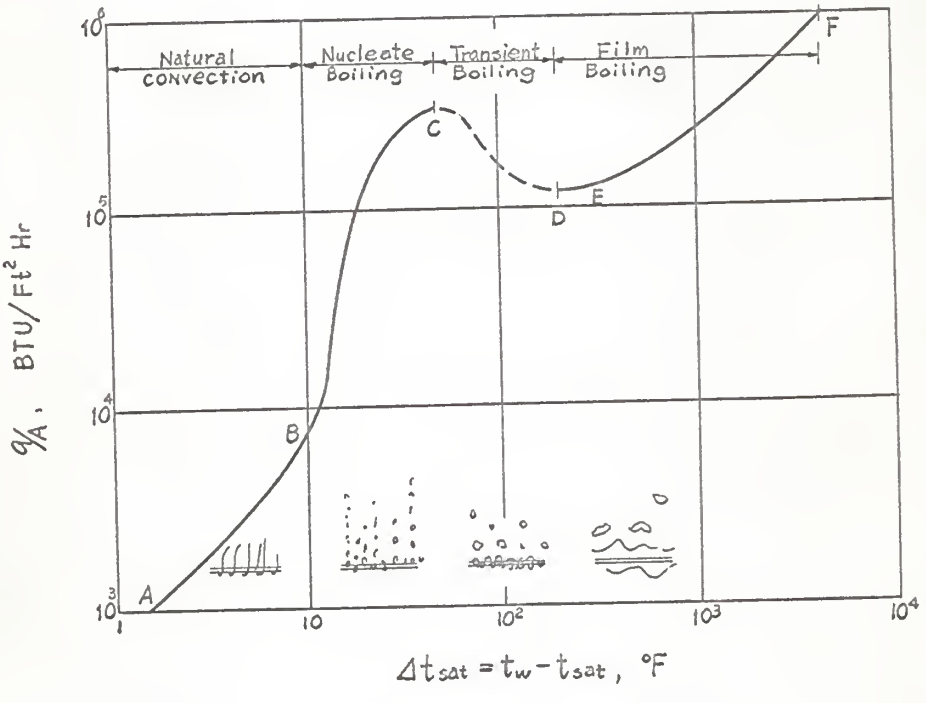

Fig. 1, Regimes of pool boiling

only from the free surface of the liquid. The condition is exactly the same as natural convection; heat flux q/A is proportional to $\Delta t^{5/4}$. In region BC, bubbles form at the active sites on the heating surface and rise through the pool; the heat flux increases very rapidly as the temperature increases; and q/A is roughly proportional to Δt^n, where n ranges from 2 to 6. This region is called nucleate boiling. At point C, the heat flux goes through a maximum, after which q/A decreases as Δt increases. This region, CD, is called the unstable or transition region, and C is the peak point or burnout point. The drop of heat flux in range CD is because most of the heating surface is covered with vapor film which prevents the conduction of heat directly to the liquid. At a point near D, the heating surface is already completely covered by a vapor film; hence region DEF is known as film boiling.

Among all of these regions, the nucleate boiling is most significant here because it transfers a large amount of heat in a moderate temperature difference. The problem in nucleate boiling is so complicated that even after 30 years of study, a correct mechanism from which some of the heat transfer problems can be predicted still has not been devised (31).

2-2. General Consideration of Bubble Dynamics

The unusual heat flux in nucleate boiling is generally believed to be the result of the ebullition of bubbles from

the heating surface. Consequently, to discuss the phenomena of nucleate boiling heat transfer, it is convenient to begin with a survey of bubble dynamics.

(a) Active Sites

Liquids have a tendency to evaporate when their intrinsic vapor pressure is greater than the surrounding pressure. But this is true only when the liquid-vapor interface is flat. On a curved interface, as in the case of a bubble, Gibbs (32) showed that the equilibrium pressures are

$$(P_v - P) = \frac{\sigma}{R_1} + \frac{\sigma}{R_2} \tag{1}$$

which reduces to

$$(P_v - P) = \frac{2\sigma}{R} \tag{2}$$

for a spherical bubble as proved by Kelvin in 1870.

From Eq. (1), it is apparent that forming a bubble from nothing (zero radius) would require an infinitely large vapor pressure. It also means that only an infinitely superheated liquid can ebulliate a bubble from a perfectly flat surface with completely distilled liquid. Hsu (33) has carried out the boiling of pure, degassed water on a thin layer of clean mercury and showed that no boiling occurred except an irregular explosive-like formation of a huge bubble due to cavitation. This perfect condition seldom exists in actual cases. In ordinary equipment, because of the nucleation sites on the

heating surface, bubbles are generated at a moderate superheat of 30F or less.

Viewing the active sites directly with a microscope, H. B. Clark and others (34) have observed that these sites are sharp, deep pits or scratches with diameters of about 0.0003 ~ 0.003 inch. It is also generally believed that these pits or scratches must contain trapped gas if they are to be capable of causing bubble generation (35).

Fig.2. Typical shapes of cavity

Consequently, shapes (C) and (D) in Fig. 2 are excellent active sites.

(b) Bubble Stability

From Kelvin's equation (2), it can easily be seen that under a constant pressure process, the process is unstable (36). Once equilibrium is established, an accidental increase of radius will reduce the required equilibrium pressure difference. If the pressure difference remains unchanged, the surplus vapor phase pressure will cause a further increase in bubble radius together with a further reduction of the required balancing pressure. This repeated action

certainly will make the growth continue without end. If a bubble contains only inert gas, an increase of radius will be followed by a decrease of pressure and the bubble will cease to grow to an appropriate size. For a vapor bubble, the pressure of the vapor inside is maintained by continuous evaporation from the surrounding liquid. Therefore, a growing bubble will keep growing as long as the liquid temperature is maintained. Similarly, a collapsing bubble will continue collapsing. For later reference, two typical cases will be discussed below.

(i) Bubbles attached to the heating surface.

As has been discussed, once a nucleus is formed, the vapor bubble becomes unstable. So, if the bulk temperature is high, as shown in Fig. 3 (a), the bubble will keep growing until a certain size is reached at which time it detaches from the surface. If the bulk temperature is not high enough, as in the highly subcooled

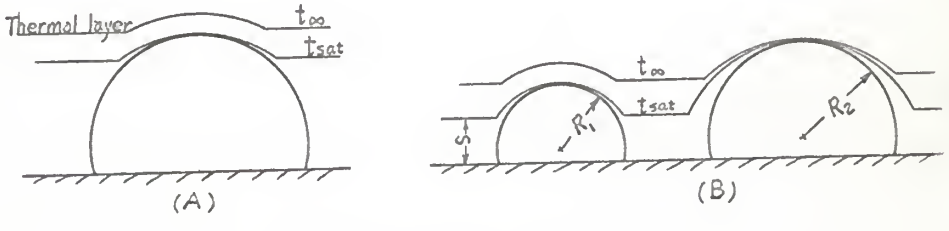

Fig. 3. Bubble growth on the wall

case, the saturation temperature thickness is less than the detaching radius, as shown in Fig. 3 (b). The bubble will first grow to a size at which the vapor condensed in the top is more than that evaporated from the bottom. When this stage is reached, the bubble collapses. Due to the inertia of the growth, the bubble will oscillage in the range between R_1 and R_2 as can be seen in a kitchen kettle. Generally it can oscillate several times without detaching from the surface.

(ii) Bubbles floating in an infinite medium.

When a bubble is floating in bulk liquid, it will continue to grow and absorb some heat from the liquid, if the liquid is in a superheated condition. But in ordinary cases, the bulk liquid seldom is superheated. If it is, the degree of superheat is generally limited to 1F or 2F. Hence it is reasonable to say that a bubble collapses more or less in the bulk liquid.

(c) Bubble Growth Rate

In order to study the stirring effect of bubbles, some considerations about bubble growth rate in the liquid are necessary. The first consideration is the modified Rayleigh equation

$$R \frac{d^2R}{d\theta^2} + \frac{3}{2} \left(\frac{dR}{d\theta}\right)^2 + \frac{2\sigma}{\rho_L R} = \frac{P_v - P}{\rho_L} \qquad (3)$$

where a term of surface tension was added to his original equation (37). Before this equation can be solved, some supplementary relations must be established. First, since most of the experiments are based on temperature, the relation between $(P_v - P)$ and $(t_w - t_{sat})$ must be clarified. In a superheated liquid, F, Romie (38) has reported that the pressure variation in the Rayleigh equation should be obtained from the Clausius-Clapeyron equation

$$(P_v - P_\infty) = \Delta P = \frac{L}{T(V_1 - V_2)} \Delta T = \frac{L}{TV_{fg}} (t_w - t_{sat})$$

Second, the heat of vaporization is due to conduction from liquid bulk to bubble surface. So there must be a relation between rate of heat conduction and bubble radius. This can be easily shown as

$$L\rho_v \frac{dV}{d\theta} = hA\Delta t \tag{4}$$

Or, for a spherical bubble, $V = \frac{4}{3}\pi R^3$, $\frac{dV}{d\theta} = 4\pi R^2 \frac{dR}{d\theta}$, hence

$$\frac{dR}{d\theta} = \frac{h\Delta t}{L\rho_v} \tag{5}$$

By using these relations, Plesset and Zwick (39) obtained a relation,

$$R = \sqrt{3} \frac{2K\Delta t}{L\rho_v (\pi\alpha)^{1/2}} \theta^{\frac{1}{2}} \tag{6}$$

which predicts that the radius increases as the square root of time. Apparently, Eq. (6), which was developed for bubble growth in an infinite medium, cannot be regarded as correct

for bubble growth on a wall. Though many authors have proposed a variety of approaches, they are too complicated to be considered in this fundamental treatment. A much simpler treatment based on a new mechanism will be discussed in Section 3 of this report.

2-3. Factors Affecting Nucleate Boiling Heat Transfer

(a) Nature of the Surface

Jakob and Fritz (1) found that a grooved copper surface adsorbed air and initially gave a much higher coefficient in the range of moderate heat flux. However, with continued boiling the coefficient decreased and very closely approached those for smooth chromium-plated surfaces. In both cases the area was taken as the projected area of the plate, regardless of the fact that the grooved surface had an actual area 1.8 times that of the smooth plate. Deutsch and Rhode (40) boiled distilled water at atmospheric pressure with high heat flux and found that, for a given Δt, the coefficient U based on the projected area was not increased by roughening the surface and that U based on the total surface was less than that for the smooth tube.

From the above experiments, it can be concluded that an artificially-roughened surface will shift the moderate heat flux part of the boiling curve based on the projected area to the low Δt end while maintaining the high heat flux part practically unchanged as in the smooth surface.

For surfaces of different materials, the data of Bonilla and Perry (12) (Fig. 4) show that for boiling ethanol at atmospheric pressure on a horizontal flat plate, a higher thermal conductivity gives higher heat flux at a given Δt, while the maximum heat flux remains practically the same for all four surfaces. But with water or methanol boiling at atmospheric pressure in a small submerged tube evaporator, Cooper and others (40) found that U was larger with iron than copper tubes, indicating that the increase in the number of vaporization nuclei had over-compensated for the decrease in thermal conductivity. Thus it can be concluded that, for different surfaces, the higher the thermal conductivity and the more the evaporization nuclei, the higher the resulting heat flux. An aged surface generally decreases both thermal conductivity and number of evaporization nuclei.

(b) Effect of increased velocity

In the range of low Δt, the use of forced convection in a boiling system results in an increase in the heat flux for a given Δt. But in the region of strong nucleate boiling, the influence of velocity is small, as shown in Fig. 5. Line A shows data of Beecher (40) for water at 212F and 1 atm flowing at 3 ft./sec. normal to an electrically heated 0.050-inch diameter stainless steel tube; Line B represents data for water boiling on a 0.048 inch platinum wire in an unstirred pool at 1 atm. It is apparent from this figure that in a

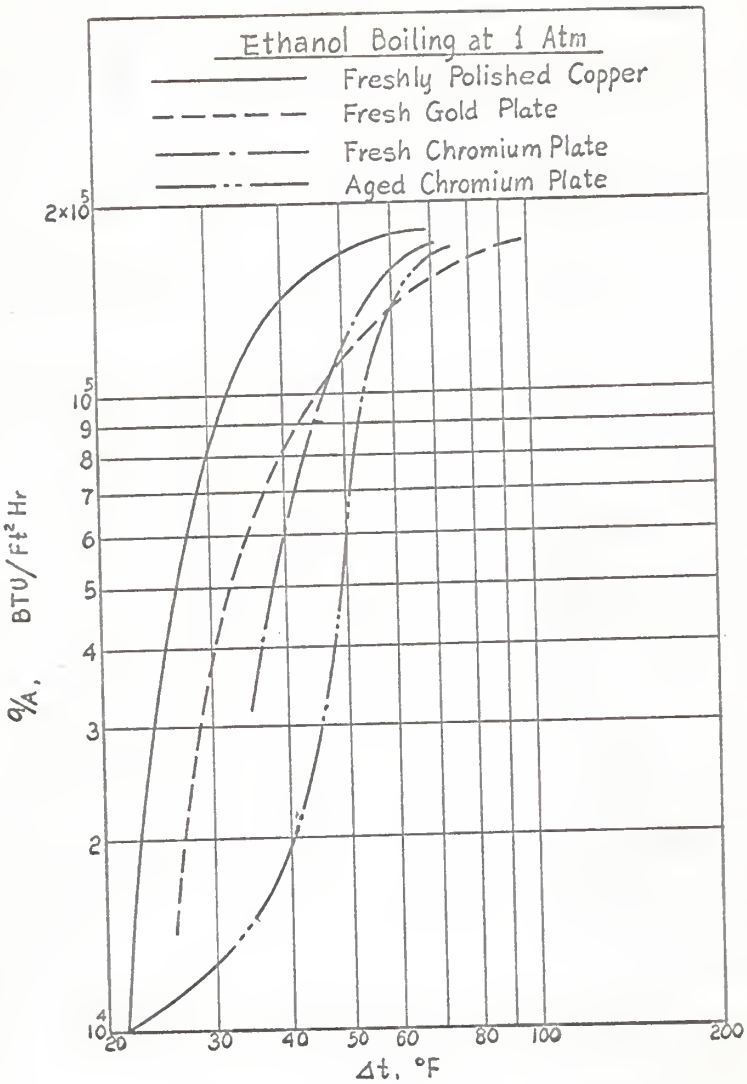

Fig. 4. Effect of heating surface (12)

strong nucleate boiling range the heat flux is essentially unaffected by mechanical agitation.

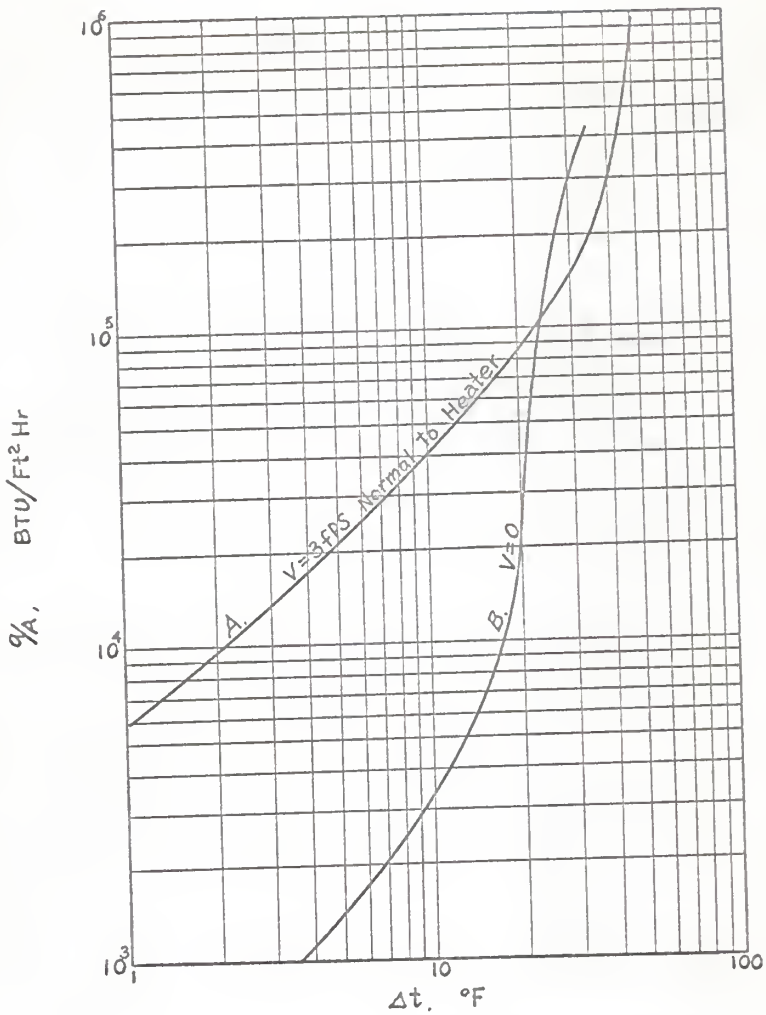

Fig.5. Effect of mechanical agitation (2)

(c) Effect of subcooling

In an ordinary heat transfer problem, the heat flux is generally proportional to the temperature driving force $(t_w - t_\infty)$, but things are always unusual whenever boiling heat transfer is concerned. Figure 6 shows a logarithmic

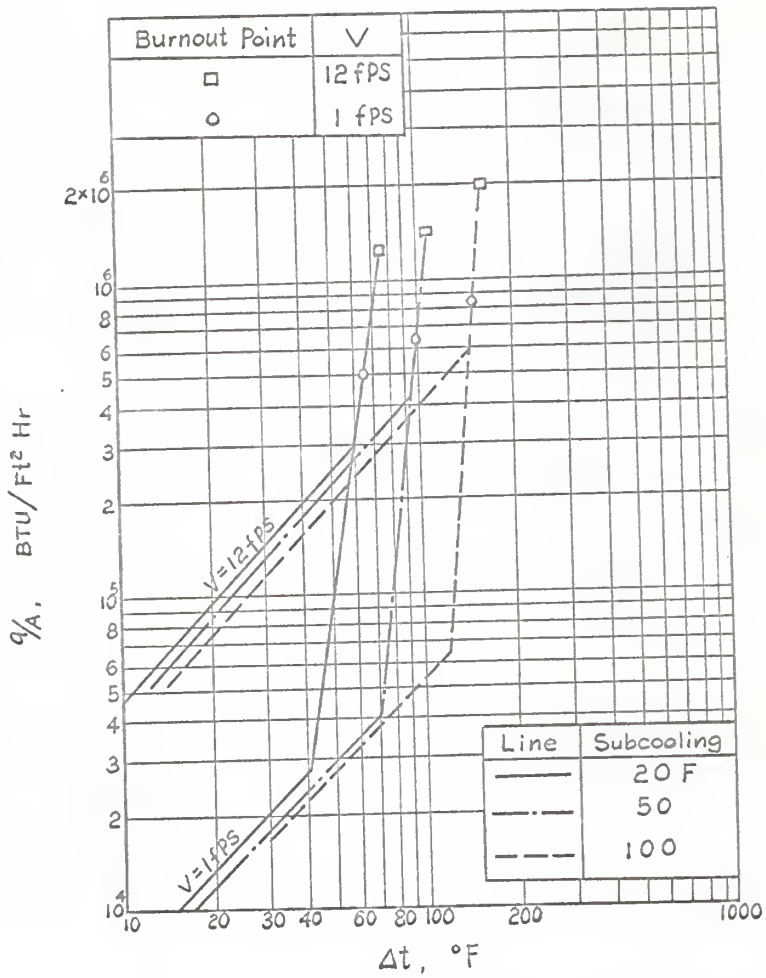

Fig. 6. Typical boiling data for subcooled forced convection (2)

graph of the heat flux q/A plotted as ordinate vs. the total Δt from heater to the degassed water. In the nonboiling region, the results for each agree with those expected from conventional equations for forced convection without change

in phase. In the local boiling region, the curves are steep and are displaced horizontally for each value of subcooling by values of Δt corresponding closely to the differences in subcooling.

When the same data for surface boiling are plotted, in a different fashion, as shown in Fig. 7, with $\Delta t_{sat} = t_w - t_{sat}$ replacing $\Delta t = t_w - t_\infty$ as abscissa, the results are insensitive to water temperature and velocity. The slope of the curve in Fig. 7 is similar to that for the boiling of a pool of saturated liquid.

(d) Effect of pressure

For a large number of liquids boiling in pools in the nucleate region at pressures of 1 atm. and less, the data show that a decrease in saturation pressure gives a lower heat flux for a given Δt (40). For pressures higher than atmospheric pressure, the data also show that an increase in saturation pressure gave a higher heat flux for a given Δt, but the peak flux is a curved line with a maximum midway to the critical state. Figure 8 shows the curve plotted from the data of Addom (3). The heat transfer coefficient at 2465 psia was 100 times greater than the value for the same Δt at 1 atm.

2-4. Some Proposed Mechanisms

Several mechanisms of nucleate boiling heat transfer have been proposed during the past three decades. They were

all suggested to correlate the data of the extremely high heat flux of nucleate boiling. Unfortunately no one of them had ever successfully explained the experimental facts stated in the preceding section.

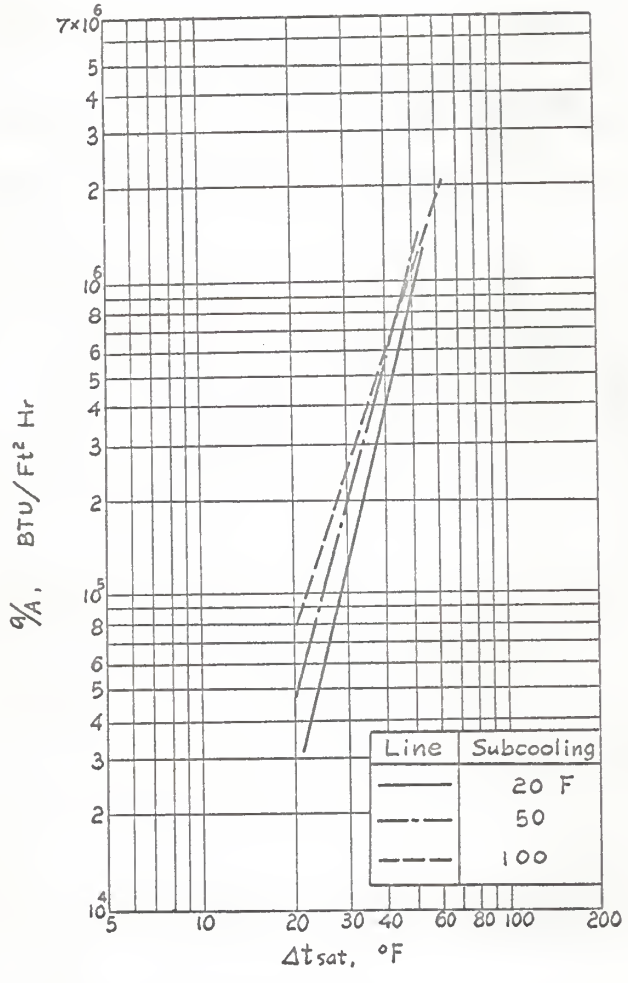

Fig. 7. Data of Fig.6 as a function of Δt_{sat}

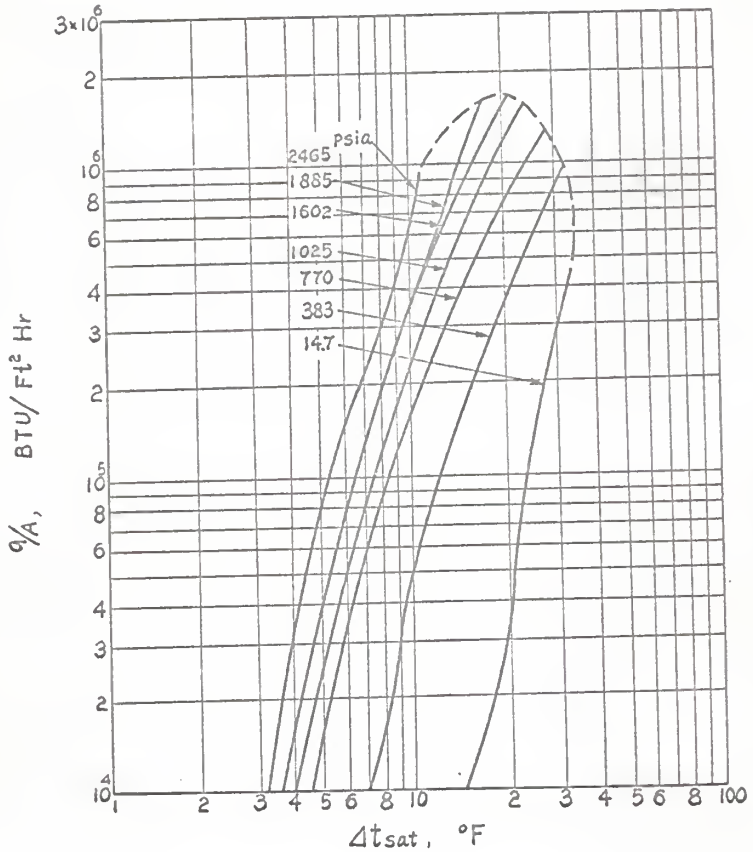

Fig. 8. Effect of pressure (3)

(a) Microconvection in the sublayer

This mechanism is most widely accepted at the present time. The heat path is assumed to lead from the heating surface to the liquid between the bubbles. Observed high heat flux is considered due to the stirring effect of the bubbles. As shown in Fig. 9, contrary to the convective velocities

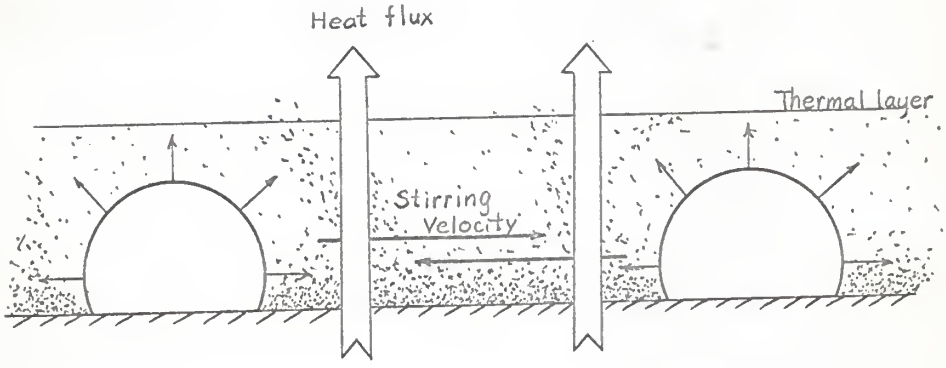

Fig. 9. Stirring effect of bubbles

that change the sublayer pattern from outer layers, the bubble growth velocities stir the liquid from inside the sublayer. Consequently, these radial velocities of the order of 10 or 20 fps are estimated so large that they determine the temperature distribution in the sublayer near the heating surface.

This mechanism, of course, provides a high heat flux in nucleated boiling if everything happens to be as described above. However, it is also very important to observe that if heat flows from the heating surface through the thermal sublayer to the bulk liquid, it depends strongly on the temperature difference ($t_w - t_\infty$) which is the driving potential of the heat flux. But as already discussed in Section 2-3, the heat flux is essentially independent of the degree

of subcooling. This proposed mechanism is not as good as originally expected.

(b) Bubbles act in the manner of surface roughness

That bubbles act in the manner of surface roughness was suggested by H. S. Tsien (31). For boiling heat transfer with forced convection, the bubbles on the heating surface increase the turbulent exchange of liquid between the heating surface and the moving bulk liquid. The effect is similar to that produced by plate roughness. But just as for the mechanism (a), the heat flux would again have to depend directly on the temperature driving force $t_w - t_\infty$. Furthermore, the turbulent exchange has nothing to do with the case of pool boiling, which, it is believed, should have the same basic mechanism as in forced convection boiling.

(c) Latent heat transported by bubbles

Latent heat transport means that while a bubble grows it absorbs the latent heat of vaporization which is then returned to the bulk liquid where the bubble collapses. By calculating the total bubbles formed and the total latent heat contained in these bubbles, Rohsenow and Clark (15), also Gunther and Kreith (16) showed that the latent heat carried by the bubble contributed only 1% or 2% of the total heat flux. It is interesting to note that both cases studied were under conditions of high subcooling of 150F and, as pointed out by Bankoff (26)

and Snyder (41), this heat flux carried by latent heat could be increased by assuming additional heat flux through the bubbles by mass transfer. That is, heat flows into the individual bubble through the superheated base near the heating plate. This heat is absorbed as heat of vaporization at the vapor-liquid boundary, and is then carried as steam to the top of the bubble where the vapor condenses and gives off latent heat to the subcooled liquid bulk. A more detailed discussion will be treated in Section 3 of this report.

(d) Vapor-liquid exchange action

This vapor-liquid exchange action was a mechanism suggested by Forster and Greif (41). The main idea is that when a bubble is formed and detaches from the heating surface or collapses above the heating surface, it pushes an amount of hot liquid having the same volume as the bubble into the liquid bulk, as shown in Fig. 10. This vapor-liquid exchange is assumed to contribute the most heat flux in nucleate

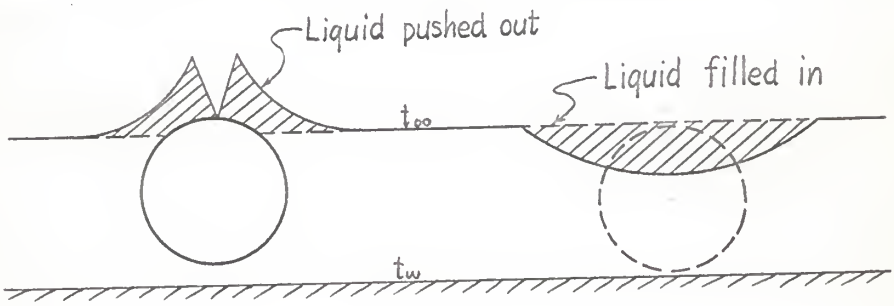

Fig. 10. Vapor liquid exchange action

boiling heat transfer. Indeed, by using the following equation, Forster and Greif (41) were able to show that the heat transferred by this vapor-liquid exchange action would contribute about 320% of the total observed heat flux.

$$\Delta H = C \rho_L \, V \Delta t_{mean} \tag{7}$$

But this only means that vapor-liquid exchange action could be a main contributer to nucleate boiling heat transfer only if the temperature difference Δt_{mean} used in Eq. (7) is correct or nearly correct. From Fig. 11, it is easily seen that when a bubble detaches from the surface or collapses over the surface, the liquid pushed into the bulk is actually the relatively low temperature part. Therefore, the temperature difference to be used in Eq. (7) should be much less than Δt_{mean}, and the contribution by this exchange should be much less than that calculated by Eq. (7).

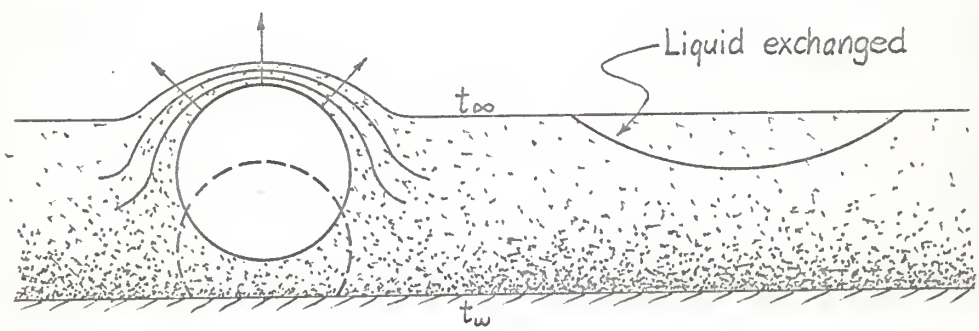

Fig. 11. Temperature of the liquid exchanged

(e) Microlayer evaporation

The most recently proposed mechanism is microlayer evaporation, as suggested by Moore and Mesler (24). By using a sensitive, plated thermocouple directly on the bubble site, Moore and Mesler observed an unusual temperature drop on the surface while the bubble was growing. From this they concluded that a microlayer exists inside the bubble, and the evaporation of this microlayer will contribute a large amount of the heat flux observed. But, as pointed out by Lyon, Fourst and Katz (42), if wetting does not occur, then the formation of a microlayer would be unlikely. Thus, nucleate boiling would not be expected if it is dependent upon microlayer vaporization.

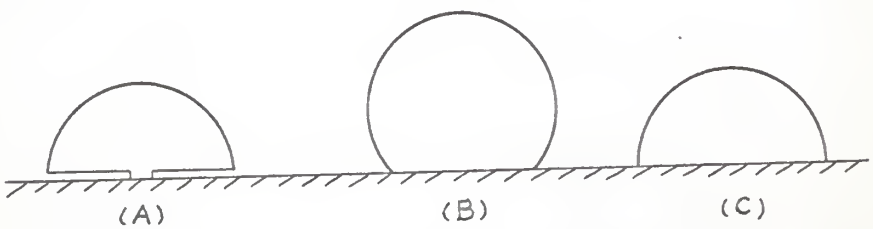

Fig. 12. Microlayer evaporation

3. TRIPLE INTERFACE EVAPORATION

Investigators constantly point out that the latent heat transport should have a major role in nucleate boiling heat transfer. However, neither an experimental method nor an analytical approach has ever been tried to give a more concrete evaluation of this process. To make things clear, an analytical study, though brief in itself, is necessary.

3-1. Contribution of Bubble Latent Heat

Gunter and Kreith (16) and Rohsenow (15) have observed that, when boiling a highly subcooled liquid, the latent heat contained in the bubbles has an order of magnitude of only 1% or 2% of the total observed heat flux. This does not necessarily mean that the heat transferred to the bubble is

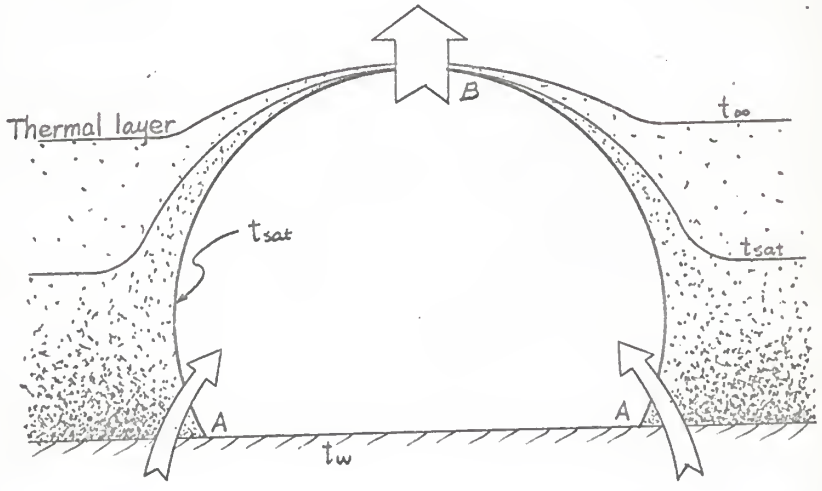

Fig. 13. Heat flux through latent heat transport

insignificant. It can be seen in Fig. 13 that when boiling a highly subcooled liquid, vapor bubbles are always larger than the thickness of thermal boundary layer (31). This explains why bubble diameters are smaller in a subcooled condition than in a saturated liquid. However, due to the high thermal diffusivity in liquid bulk, the thermal layer on top of the bubble can be expected to be very small. Across this extremely thin thermal layer, the temperature driving force is $t_{vap} - t_{liq} = t_{sat} - t_{\infty}$ = degree of subcooling. Consequently, the latent heat contained in the bubble itself may be of a small order of magnitude. The heat flux transferred to the bulk liquid through the top of the bubble in a highly subcooled condition is undoubtedly of very large magnitude. To check the possibility, Fig. 13 shows that if heat flux passing through B is very large, the heat flux through A into the bubble should also be very large. Because the temperature difference is the same $(t_w - t_{sat})$ for both subcooled and saturated cases, the heat flux passing through A should remain practically the same for both cases. (This can be considered as a reasonable assumption for the time being and will be proved later). Furthermore, in the saturated case $t_{vap} - t_{bulk} = t_{sat} - t_{sat} = 0$, the heat flux through B should be zero. All the heat flux through A must equal the latent heat of vaporization of the vapor contained in the bubble. This indicates that if one can find a large amount of heat carried by the vapor contained in the bubble when boiling

saturated liquid, it can be concluded that the latent heat transport at the top of bubble is significant when subcooled liquid is boiled. This is the actual case if a brief calculation is made from the data of Westwater and Santangelo (29).

(A) Data of Westwater and Santangelo:

. Liquid: methanol at 1 atm

. Observed overall coefficient: $U = 1350$ BTU/hr ft^2F

. Overall temperature difference: $\Delta t = 70F$

. Average bubble size: $d = 0.17$ inch diameter

. Bubbling rate: $f = 17$ bubbles/sec.

. Spacing of nuclei sites = 0.103 inch

(B) A calculation based on one square foot:

. Total nuclei site $= \frac{12}{0.103} \times \frac{12}{0.103} = 14400$

. Total number of bubbles leaving heating surface per hour $= 14400 \times 17 \times 60 \times 60 = 8.8 \times 10^8$

. Volume of one bubble $= \frac{3.14 \times 0.17^3}{6} = 0.00257$ in^3

$= 1.485 \times 10^{-6}$ ft^3

Specific volume of CH_3OH at saturation (43)

$= 13.05$ ft^3/lb

. Mass of one bubble $= \frac{1.485 \times 10^{-6}}{13.05} = 1.138 \times 10^{-7}$ lbs

. Latent heat of $CH_3OH = 482$ BTU/lb at 1 atm.

. Total heat carried by bubbles

$= 482 \times 1.138 \times 10^{-7} \times 8.8 \times 10^8$

$= 48200$ BTU/hr $ft^2 = 688$ BTU/hr ft^2 F

. Percentage of observed heat flux carried by detaching bubble is $\frac{688}{1350} = \underline{52\%}$

This is the precentage contributed by bubble latent heat in a condition still much below the peak condition. At peak flux, q/A = 172,000 BTU/hr ft^2, the percentage will be still more.

The high heat content of a vapor bubble also can be easily visualized in ordinary high-duty power boilers. In a power boiler as shown in Fig. 14, all the heat absorbed from the heating surface is used to generate saturate steam. If

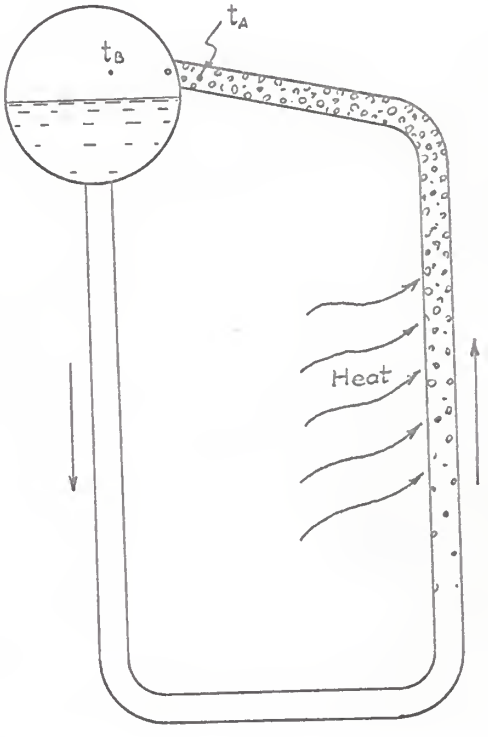

Fig. 14. Schematic diagram of power boiler

the steam is generated by evaporation from the free surface, then owing to the large amount of heat absorbed in evaporation, the temperature at A should be much higher than the saturate steam temperature at B. However, the temperature at A differs only slightly from t_B as can be seen from any boiler operating data (44). From this fact, it is reasonable to say that the steam to be generated has already become steam while still inside the boiler tubes. This certainly means that the absorbed heat has gone entirely to the bubbles.

Although only the case of boiling a saturated liquid is discussed here, it will be proved later that the condition is the same when a subcooled liquid is boiled.

3-2. Triple Interface Evaporation

The high heat flux carried away by bubbles when boiling a saturated liquid has already been discussed. The next step is to find how such a large amount of heat can flow into the bubbles. A general discussion of interface heat transfer follows. From the kinetic theory of gases and liquids, it is known that liquid molecules evaporate continuously whenever the surrounding pressure is less than the intrinsic vapor pressure of the liquid. (Of course, only net evaporation is of interest here.) Also, the latent heat carried away by this evaporation is so fast that, when compared with the heat rate conducted from the liquid bulk, it can be considered as infinite. This infinite heat transfer coefficient

is actually an assumption adopted by most authors when treating the bubble growth rate in boiling (33) (45). Experimentally, Alty (46) also observed that when reducing the vapor phase pressure, a water droplet temperature of 25C was able to form a thin layer of ice on the surface. For a numerical concept, it is known that the maximum rate of evaporation of a liquid evaporating to a vacuum is equal to the rate of the vapor molecules that would collide on the liquid surface if the vapor is at saturation pressure. More precisely, it equals the vapor molecules that are colliding on the liquid surface and have been captured. Thus, the maximum rate of evaporation to vacuum can be expressed as (47)

$$\dot{m} = \tfrac{1}{4} f P \sqrt{\frac{8M}{\pi RT}} \qquad (8)$$

where f is a factor taking care of the molecules that collide with but are not captured by the liquid. The value of f differs from liquid to liquid. For most liquids, however, it is very close to unity but for water at 212F it was shown by Alty (46) that f has a value of only 0.04. Therefore, for water at 212F, Eq. (8) becomes

$$\dot{m} = 0.01 P \sqrt{\frac{8 \times 18}{3.14 \times 49750 \times T}} \text{ (slugs/ft}^2\text{, hr)}$$

or

$$\dot{m} = 0.00975P \sqrt{\frac{1}{T}} \text{ (lbs/ft}^2\text{, hr)} \qquad (9)$$

For water at 248F evaporating to a vapor space of 1 atm, the net rate of evaporation is:

$$\dot{m}_1 - \dot{m}_2 = 0.00975 \times 144 \left(28.797 \sqrt{\frac{1}{708}} - 14.7 \sqrt{\frac{1}{672}}\right)$$
$$= 2510 \text{ lbs/ft}^2, \text{ hr}$$

The latent heat carried by this evaporated vapor is

$$q/A = 2510 (1150.4 - 216.45) = 2.34 \times 10^6 \text{ BTU/ft}^2 \text{ hr}$$

This shows that for a temperature difference of 36F at 1 atm. the heat flux carried by evaporation is 5 times as much as the peak flux observed in nucleate boiling. This also shows that if 20 percent of the area goes through an evaporation process, it will result in a heat flux equivalent to the maximum heat flux in nucleate boiling.

A physical picture of the bubble heat transfer process is now in order. In treating the growth rate of bubbles, Griffith (45) assumed the boundary conditions of a growing bubble as shown in Fig. 15 (A). In this figure, there is a

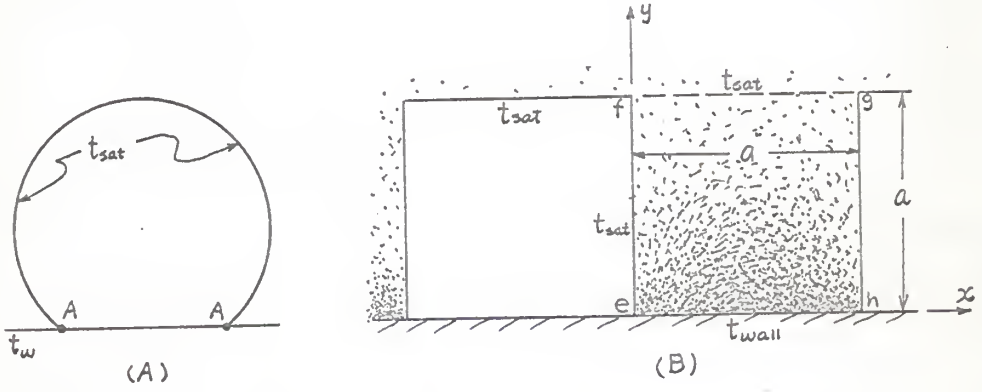

Fig. 15. Discontinuity in triple interface

discontinuous point called the triple interface (or line) A. At this point, it is obvious that the temperature gradient across the corner is infinite. Thus, if the condition is good enough, the heat rate through the neighborhood of A can be infinite in magnitude. To check the behavior of this region, a simplified stationary two-dimensional square bubble is assumed as shown in Fig. 15 (B). Although the actual bubble is growing, unsteady and spherical, the simplified bubble does provide a good approximation so far as the qualitative behavior of the corner is concerned. The steady temperature distribution in the square liquid e-f-g-h has been solved by Carslaw and Janger (48) as

$$t-t_{sat}=\frac{4(t_w-t_{sat})}{\pi}\sum_{n=0}^{\infty}\frac{1}{(2n+1)}\,\mathrm{Sin}\,\frac{(2n+1)\pi x}{a}\,\mathrm{Sinh}\,\frac{(a-y)(2n+1)\pi}{a}\,\mathrm{Cosech}\,(2n+1)\pi$$

In order to calculate the heat flow to the vapor phase, the above equation must be differentiated to find the temperature gradient at x=0. But the termwise differentiation is not allowed because in differentiating the above equation term by term results in

$$\frac{\partial t}{\partial x}=\frac{4(t_w-t_{sat})}{\pi}\sum_{0}^{\infty}\frac{\pi}{a}\,\mathrm{Cos}\,\frac{(2n+1)\pi x}{a}\,\mathrm{Sinh}\,\frac{(a-y)(2n+1)\pi}{a}\,\mathrm{Cosech}\,(2n+1)\pi$$

or

$$\left.\frac{\partial t}{\partial x}\right|_{x=0}=\frac{4(t_w-t_{sat})}{a}\sum_{0}^{\infty}\mathrm{Sinh}\,\frac{(a-y)(2n+1)\pi}{a}\,\mathrm{Cosech}\,(2n+1)\pi \qquad (10)$$

which does not converge at y=0. But a little rearrangement shows that Eq. (10) converges uniformly in the interval

$\delta \leq y \leq a$, where $\delta > 0$. (See Appendix 1.) Thus the termwise differentiation is valid for this interval.

For $\delta \leq y \leq a$, the heat flow from liquid phase to vapor phase is

$$Q_{\delta\text{-}a} = \int_{\delta}^{a} K \frac{\partial t}{\partial x}\Big|_{x=o} dy$$

$$= \frac{4K(t_w - t_{sat})}{\pi} \sum_{o}^{\infty} \frac{1}{(2n+1)} \left[1 - \operatorname{Cosh} \frac{(a-\delta)(2n+1)\pi}{a}\right] \operatorname{Cosech}(2n+1)\pi \quad (11)$$

By proper simplification, some values of $Q_{\delta\text{-}a}$ are calculated in Appendix 2. The general behavior of the triple interface discontinuity is shown in Fig. 16. From this figure, it is apparent that the heat flow into the vapor phase is infinite. Also, it is shown that this heat flux is mostly contributed by the slim area near the bubble base that is in contact with the heating surface. This is, of course, an ideal case that would not occur because of the meaningless infinite heat flux. But it is true that the heat flux distribution in an actual case should resemble the distribution of that shown in Fig. 16. That is, the heat flow into the bubble occurs mostly over the small region of the liquid-vapor-solid triple interface. Since the condition near the triple interface should be the same for both saturated and subcooled cases when t_w remains the same, the heat flow into the bubble also should be the same under the same t_w and t_{sat}.

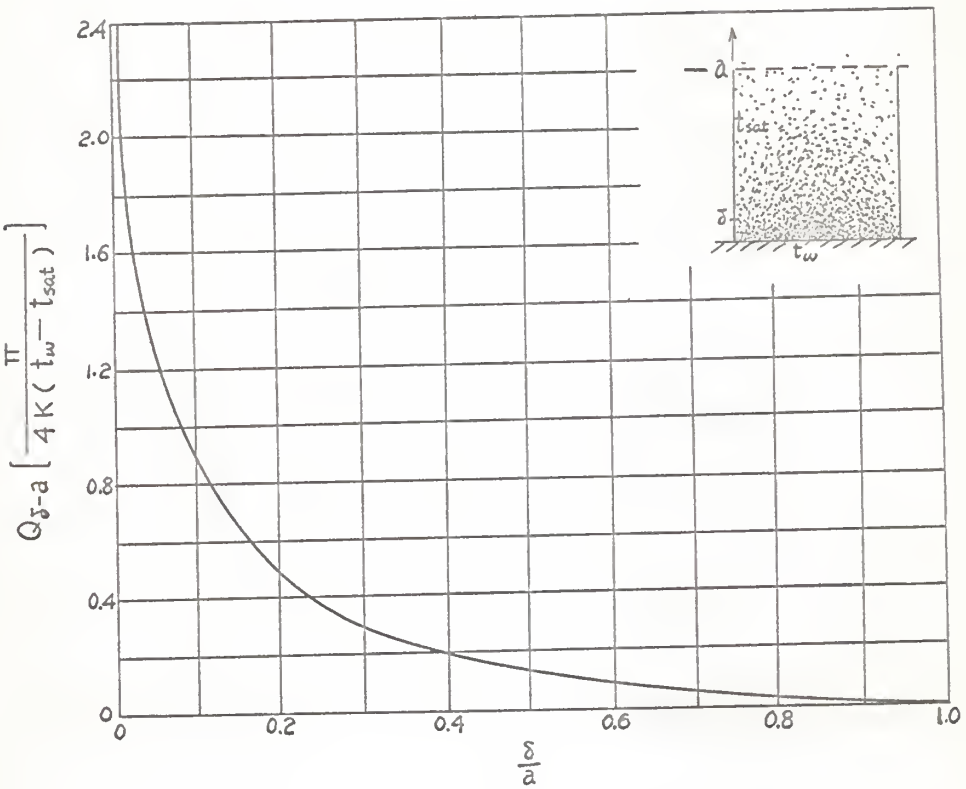

Fig. 16. General behavior of triple interface discontinuity

For an experimental proof of this extreme heat flux at the discontinuity, it is interesting to take a look at Costello and Redeker's (49) experiment. By using capillary wicking as shown in Fig. 17. Costello and Redeker have observed an amazing heat flux that is far more than that obtained by ordinary pool boiling. Although the authors did not state definitely the cause of this high heat flux, a

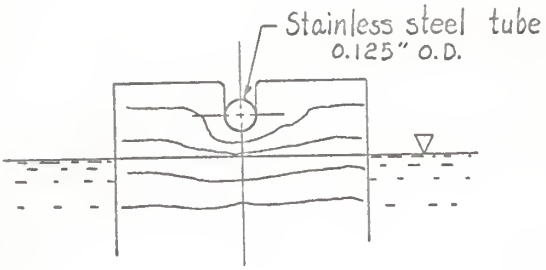

Fig. 17. Capillary wicking (49)

tentative conclusion may be that the capillary wicking process provided two solid-liquid-vapor intersection lines along the longitudinal direction of the tube.

Further proof of this discontinuous behavior is a very sharp temperature drop which should be observed at the heating surface as the bubble boundary passes through. This is due to the very high heat flux over the extremely small area at the base of bubble. This is precisely the case observed by Moor, Robers and Mesler (24) (27). Meanwhile, the assumption of microlayer evaporation seems unnecessary.

3-3. Bubble Growth Rate and Correlation of Heat Flux

In the preceding, the extreme behavior of the triple interface has been discussed. For a mathematical representation, it would be convenient to assume an effective thickness δ, within which liquid evaporates through the whole temperature driving force $t_w - t_{sat}$, and the contribution is

completely neglected beyond this thickness. Similar to the mixing length assumed in the turbulent flow problems, it is hoped that this effective thickness will be a constant or at most dependent on the saturation temperature only. In this preliminary treatment, it will be considered as constant. The magnitude of δ for water is about $\frac{1}{40}\, d_o$ (Appendix 3). Now the instantaneous area of a bubble can be written,

$$A = \pi\, d_c\, \delta \tag{12}$$

where d_c is the instantaneous contact diameter.

To find the evaporation rate through the effective area, Eq. (9) can be used. However, because this equation involves two independent variables, P and T, another means of expression is preferable. From the kinetic theory of liquids, it is known that the rate of evaporation is proportional to the number of molecules having kinetic energy greater than their bonding energy. Thus, for a liquid following the Boltzmann energy distribution, its evaporation rate to a vacuum can be expressed as,

$$\dot{m}_1 = a \exp\left(-\frac{\epsilon_o}{kT}\right) \tag{13}$$

or, since $N\epsilon_o = L$, $Nk = R$, Eq. (13) also can be written as

$$\dot{m}_1 = a \exp\left(-\frac{L}{RT}\right) \tag{14}$$

where "a" is a proportionality constant. For evaporation to bubble, the net rate of evaporation is

$$\dot{m} = a \left[\exp\left(-\frac{L}{RT_w}\right) - \exp\left(-\frac{L}{RT_{sat}}\right) \right] \qquad (15)$$

In the practical case, Eq. (15) is still very difficult to apply. When Δt_{sat} is small compared with T_{sat}, this equation can be simplified as,

$$\dot{m} = a \frac{L}{RT_{sat}^2} \exp\left(-\frac{L}{RT_{sat}}\right) \Delta t_{sat} \qquad (16)$$

which shows that the evaporation rate per unit area is approximately proportional to the first power of the temperature difference, but differs from temperature to temperature. A word of caution, usually Eq. (16) is not a good approximation because Δt_{sat} may become very large in which case Eq. (15) should be used instead.

Consider a bubble with a contact angle β, shown in Fig. 18. Let the bubble radius increases dr during a time interval $d\theta$. Since the evaporated vapor should be equal in volume to the bubble volume increase, the following should result.

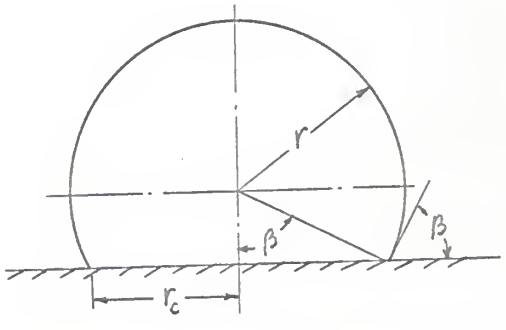

Fig. 18. Bubble growth on the wall

$$\frac{1}{\rho_v}\pi d \sin\beta\,\delta a \frac{L}{RT_{sat}^2} \exp\left(-\frac{L}{RT_{sat}}\right)\Delta t_{sat} d\theta = 2\pi r^2(1+\cos\beta)dr$$

or
$$\frac{dr}{d\theta} = \frac{\delta a L \exp\left(-\frac{L}{RT_{sat}}\right)\Delta t_{sat}}{r\,\rho_v\,RT_{sat}^2} \tan\frac{\beta}{2}$$

That is,
$$\frac{dr}{d\theta} = \frac{b}{r}\tan\frac{\beta}{2} \tag{17}$$

where
$$b = \frac{a\delta L \Delta t_{sat}}{\rho_v\,RT_{sat}^2} \exp\left(-\frac{L}{RT_{sat}}\right)$$

Integrating Eq. (17) gives
$$r = \sqrt{2b\tan\frac{\beta}{2}}\;\theta^{\frac{1}{2}} \tag{18}$$

which shows that, for a given contact angle , the bubble radius is proportional to the square root of time. This has been shown by many authors using completely different mechanisms. In an actual case, once the bubble begins to grow, the heating surface temperature will fall considerably. Therefore, the actual growth rate should be a little slower than that shown in Eq. (18). In a particular bubble, Westwater (50) observed that r is proportional to $\theta^{0.45}$. For a different contact angle, it is found from Eq. (18) that although the relation between radius and time remains the

same, the constant of proportionality increases with an increase of contact angle. That is, the bubble growth rate is higher for a semi-spherical bubble than for a spherical bubble. This fact has been observed by Johnson, Jr. and others (30), though the observers have a different explanation for it. For simplicity, the rest of this report will consider only the semi-spherical bubble, that is $\beta = \pi/2$, or $d_c = d$.

Before Eq. (12) can be applied to calculate an average effect of the heat flux, the mean effective bubble diameter d^* must be found. Since bubble diameter changes constantly, the mean effective diameter may be defined as

$$d^* = \frac{1}{\theta_o} \int_o^{\theta_o} d \, d\theta$$

Substituting Eq. (18) gives

$$d^* = \frac{1}{\theta_o} \int_o^{\theta_o} 2\sqrt{2b}\, \theta^{\frac{1}{2}} d\theta = \frac{2}{3} d_o \qquad (19)$$

where d_o is the detaching bubble diameter.

From Eqs. (12), (16) and (19) the total heat flux due to nucleate boiling can be written as

$$q/A = a N \pi d^* \delta \, \frac{L}{RT_{sat}^2} \exp\left(-\frac{L}{RT_{sat}}\right) \Delta t_{sat} \, L$$

or

$$q/A = \frac{2}{3} a \delta \pi \, N d_o \, \frac{L^2}{RT_{sat}^2} \exp\left(-\frac{L}{RT_{sat}}\right) \Delta t_{sat} \qquad (20)$$

Initially the heat flux seems proportional to the first order of Δt_{sat}, but this is not true since bubble number N increases

very rapidly as temperature increases.

Gaertner and Westwater (51) adopted a nickel-plating method and found that heat flux varies approximately with the square root of the active site population. Also, the jamming effect (33) and the high rushing velocity of evaporating vapor in a high superheat state causes the detaching bubble diameter (or aureole diameter) to decrease with an increase of superheat. Figures 19 and 20 are two rearranged curves from Figs. 7 and 13 of Gaertner and Westwater's paper.

From Fig. 19, the relation between the detaching bubble diameter and the active site population in the high heat flux range is found as

$$d_o = \frac{\eta}{N^{0.68}} \tag{21}$$

The detaching diameter d_o remains roughly the same when heat flux is small.

From Fig. 20, the relation between Δt_{sat} and active site population is obtained as

$$\Delta t_{sat} = \gamma N^{0.081} \tag{22}$$

Then from Eqs. (20), (21) and (22), the following equations result:

(a) At low heat flux:

$$q/A = \frac{2}{3} a \delta \pi N d_o \frac{L^2}{RT_{sat}^2} \exp\left(-\frac{L}{RT_{sat}}\right) \gamma N^{0.081}$$

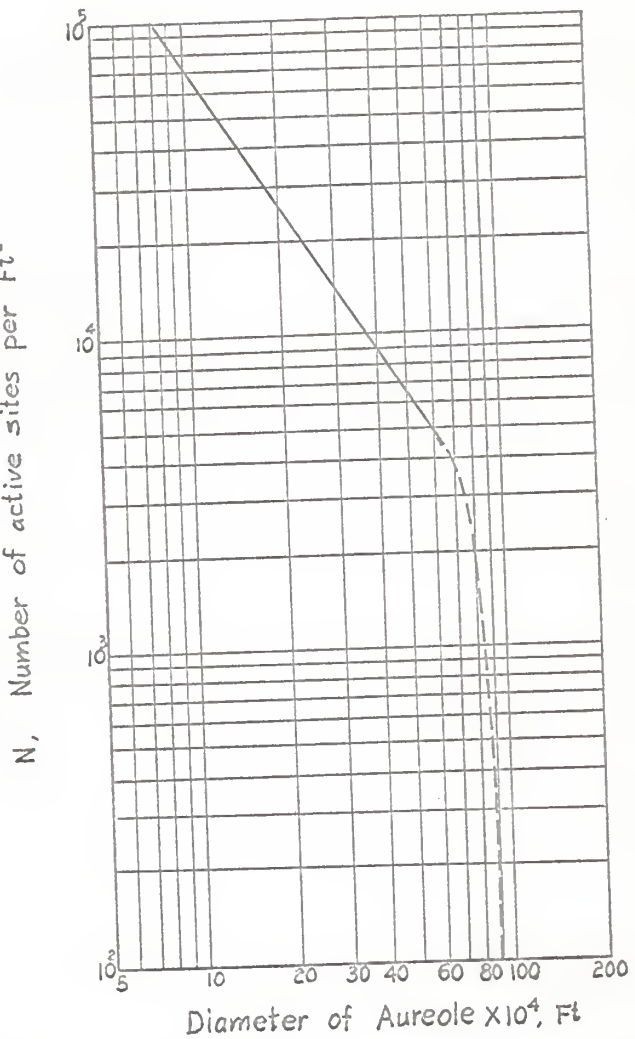

Fig. 19. Variation of detaching diameter with population (51)

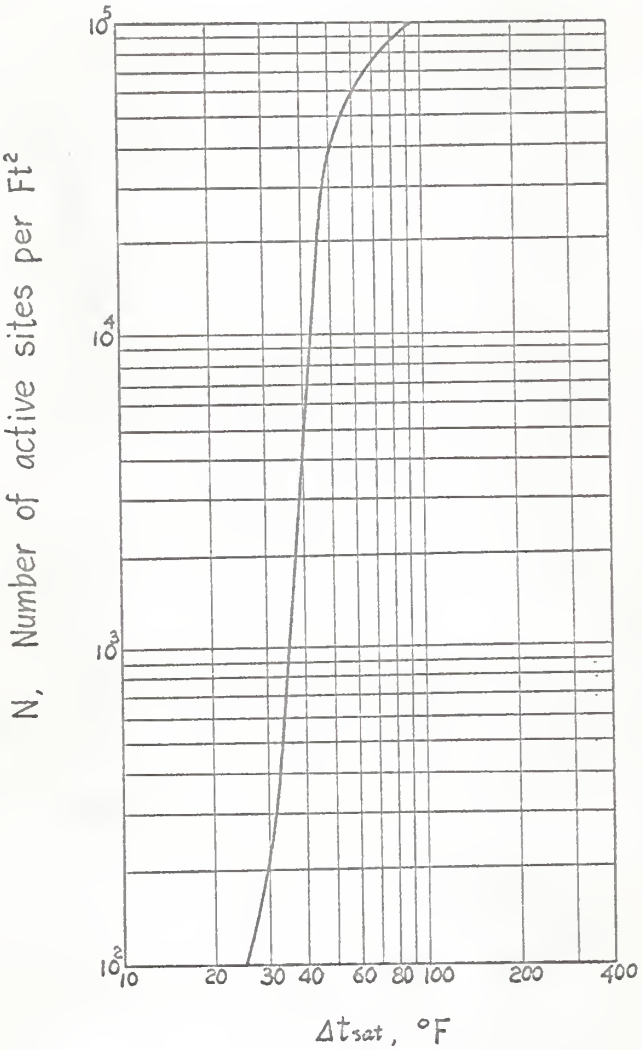

Fig. 20. Relation between superheat and bubble population

or $$q/A \propto N^{1.081} \tag{23}$$

which shows that heat flux is roughly proportional to the active site population as observed by Jakob (52).

(b) At high heat flux:

$$q/A = \frac{2}{3} a \delta \pi_N \frac{\eta}{N^{0.68}} \frac{L^2}{RT_{sat}^2} \exp\left(-\frac{L}{RT_{sat}}\right) \gamma N^{0.081}$$

or $$q/A \propto N^{0.401} \tag{24}$$

which agrees with the experiment of Gaertner and Westwater.

If the heat flux is expressed by the term Δt_{sat} only, Eq. (24) becomes

$$q/A \propto \left[\left(\frac{\Delta t_{sat}}{\gamma}\right)^{\frac{1}{0.081}}\right]^{0.401}$$

That is,

$$q/A \propto (\Delta t_{sat})^5 \tag{25}$$

for this particular case.

From the above verification, it is seen that Eq. (20) agrees very well with the experiments. But since it should be expressed in terms of active site population and detaching bubble diameter, no simple relation between heat flux and Δt_{sat} can be deduced without a knowledge of active site variation and bubble diameter behavior. This fact may be

considered as the cause of the scattering of the experimental results.

3-4. Maximum Flux and Factors Affecting Nucleate Boiling Heat Transfer

Equation (20) shows that at a given temperature, heat flux is proportional to bubble population N, bubble diameter d_o and temperature driving force Δt_{sat}. Since d_o does not change very much with Δt_{sat}, heat flux will generally increase as N increases. But this is true only when each bubble is geometrically independent. When N reaches a value at which the boundaries of the bubble begin to eclipse each other, the effective circumference per bubble will be reduced considerably. Certainly, if this reduction cannot be compensated for by the increase of N, the heat flux will then decrease in spite of the fact that wall temperature is kept increasing. This is the transition region defined by the triple interface evaporation mechanism; the turning point is know as the burnout point.

To find the peak flux, it is necessary to know the geometrical distribution of the bubbles. Artificially the maximum number of bubbles that can be packed without their boundaries touching each other is the quantity obtained by Fig. 21 (A). This is the well-known hexagonal packing. The ratio of the bubbles obtained by this hexagonal packing to that of ordinary square packing is $a/b = 1/\sin 60^\circ = 1.15$. Though

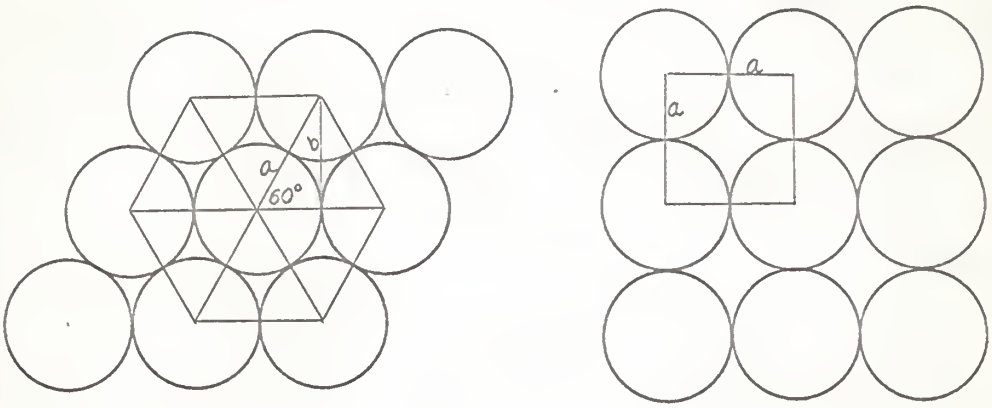

(A) Hexagon (B) Square

Fig. 21. Bubble packaging

the bubbles as arranged in Fig. 21 (A) are not necessarily the ones that give the maximum heat flux, it is very reasonable to assume that the maximum heat flux happens when the mean effective diameters are arranged as shown. From this postulate, the following equation results at burnout point:

$$N' = 1.15\left(\frac{1}{d^*}\cdot\frac{1}{d^*}\right) = 1.15\left(\frac{9}{4}\cdot\frac{1}{d_0^2}\right)$$

$$d_0' = \frac{3}{2}\,d^* = 1.05\left(\frac{3}{2}\cdot\frac{1}{\sqrt{N'}}\right) \tag{26}$$

Substituting Eq. (26) into Eq. (20) yields

$$(q/A)_{max} = 1.05\, a\delta\pi\sqrt{N'}\;\frac{L^2}{RT_{sat}^2}\exp\left(-\frac{L}{RT_{sat}}\right)\Delta t'_{sat} \tag{27}$$

or, in terms of d'_o,

$$(q/A)_{max} = 1.725\, a\delta\pi \frac{1}{d'_o} \cdot \frac{L^2}{RT^2_{sat}} \exp(-\frac{L}{RT_{sat}})\Delta t'_{sat} \quad (28)$$

Before these equations can give the exact value of the heat transferred, a, δ, d'_o and Δt_{sat} should be determined either experimentally or by statistical methods. However, these equations are already sufficient to be used to predict the qualitative effect of one factor upon the others. Some of these effects are discussed below.

(a) Effect of Subcooling

Most of the mechanisms proposed have a heat flux depending strongly on the subcooling. This is not the case in nucleate boiling as revealed in many experiments. On the contrary, the triple interface evaporating mechanism shows that heat flux in nucleate boiling depends on the superheat $\Delta t_{sat} = t'_w - t_{sat}$ only. From Eq. (20), although bubble population N and diameter d also play important roles, the bubble population can be considered as constant for a given wall temperature because it depends only on the temperature of the liquid that is in contact with the wall. However, as the bubble diameter decreases with the increase of subcooling, the heat flux contributed by nucleate boiling will be expected to be less in a high subcooled liquid. This decrease combines

with the increase of the part contributed by stirred convection will give an observed heat flux highly insensitive to the degree of subcooling.

For a given pressure, bubble diameter d_o' is smaller in a higher subcooled condition, and a smaller d_o' will make a greater $\Delta t_{sat}'$ since more bubbles are required to reach the burnout point where maximum heat flux is concerned. Taking these facts into consideration, Eq. (28) shows that subcooling should increase $(q/A)_{max}$.

(b) Effect of velocity

In the region of strong nucleate boiling, the influence of velocity is small. This can be explained in the same way as in the preceding. Since the convective velocity is not able to change the temperature of the liquid in contact with the wall, bubble population N will remain unaffected. Furthermore, because of the unstable force resulting from the velocity, bubble diameter d_o is going to be decreased as velocity increases. Then the heat flux reduction due to this decrease of bubble diameter is compensated for by the increase due to forced convection. This again will make the total heat flux highly independent of velocity. Also the maximum heat flux can be increased by increasing velocity to a certain extent.

(c) Effect of the thermal conductivity of heat transfer surface material.

In many other mechanisms, heat is assumed to flow through the whole part of the heating surface that is not covered by bubbles and the thermal conductivity can be generally neglected in comparison with the very low conductivity of liquid. But in this new mechanism, heat flows through a very narrow area near the triple interface. Thermal conductivity is essential, as can be judged from the rapid cooling effect observed by Moore and Mesler (24).

Because of the cooling effect of triple interface evaporation, the actual $(\Delta t_{sat})_{act}$ (locally near the bubble) is different from the observed Δt_{sat} (average of the whole surface). The difference $\Delta t_{sat} - (\Delta t_{sat})_{actual}$ is naturally dependent on thermal conductivity. Higher conductivity has a lower cooling effect, thus a small difference between actual Δt_{sat} and observed Δt_{sat}. From this it can be concluded that for a given observed Δt_{sat}, a higher thermal conductivity will give higher heat flux.

Since the effect of conductivity only shifts an observed temperature scale to an actual scale, the maximum heat flux is not affected. Of course, for a low conductive heater, more observed Δt_{sat} is required to attain the same amount of maximum heat flux.

(d) Effect of surface tension

For small values of surface tension, the bubble is excited at less Δt_{sat}. That is for a given Δt_{sat}, the lower the surface tension the higher the heat flux. But as the low surface tension liquid reaches its burnout point in a smaller $\Delta t'_{sat}$, a lower peak heat flux would result.

(e) Effect of pressure and temperature

Although the effect of pressure and temperature seems to be two different things, in the triple interface evaporation mechanism it can be considered as only one factor. This is because only the saturation temperature which is determined by the pressure is of concern.

The effect of pressure and temperature concerns surface tension, latent heat and temperature. For a given liquid, of course, there are definite relations between surface tension and temperature and between latent heat and temperature. But these are only in experimental forms. Equation (28) can be further simplified by substituting some typical relations between d'_o, $\Delta t'_{sat}$ and some known parameters such as surface tension, specific volume, gravitational acceleration, etc. For preliminary treatment of the new mechanism, however, Eq. (28) will remain as given and a qualitative discussion of the influence of pressure and temperature will be given.

From Eq. (20), the temperature term

$$\frac{L^2}{RT_{sat}^2} \exp\left(-\frac{L}{RT_{sat}}\right)$$

varies exponentially with absolute temperature. Figure 22 (A) shows the case of water whose heat transfer coefficient at 1000 R (962.5 psia) is known to be 200 times greater than the value for the same Δt_{sat} at atmospheric pressure if the effect of N and d_o is neglected temporarily. Since the surface tension decreases as temperature increases, the bubble population increases while the detaching bubble diameter decreases with the increase of temperature. Experimentally the variation of population is much more than the variation in diameter. Thus if the effect of N and d_o is considered, a still higher coefficient will result in the high temperature range.

For maximum heat flux, since the surface tension diminishes gradually to zero at the critical state, the $\Delta t'_{sat}$ required to reach the peak flux also diminishes due to the ease of vaporization. Qualitatively the product of $\sqrt{N'}\,\Delta t'_{sat}$ can be expressed as in Fig. 22 (B). From Eq. (27) and Figs. 22 (A) and (B), it can be seen that the maximum heat flux in nucleate boiling first increases with the increase of pressure until a certain value is reached. It then drops gradually to zero at the critical pressure.

As a summary of the above discussion, the results of these conclusions are plotted in Fig. 23. From this figure

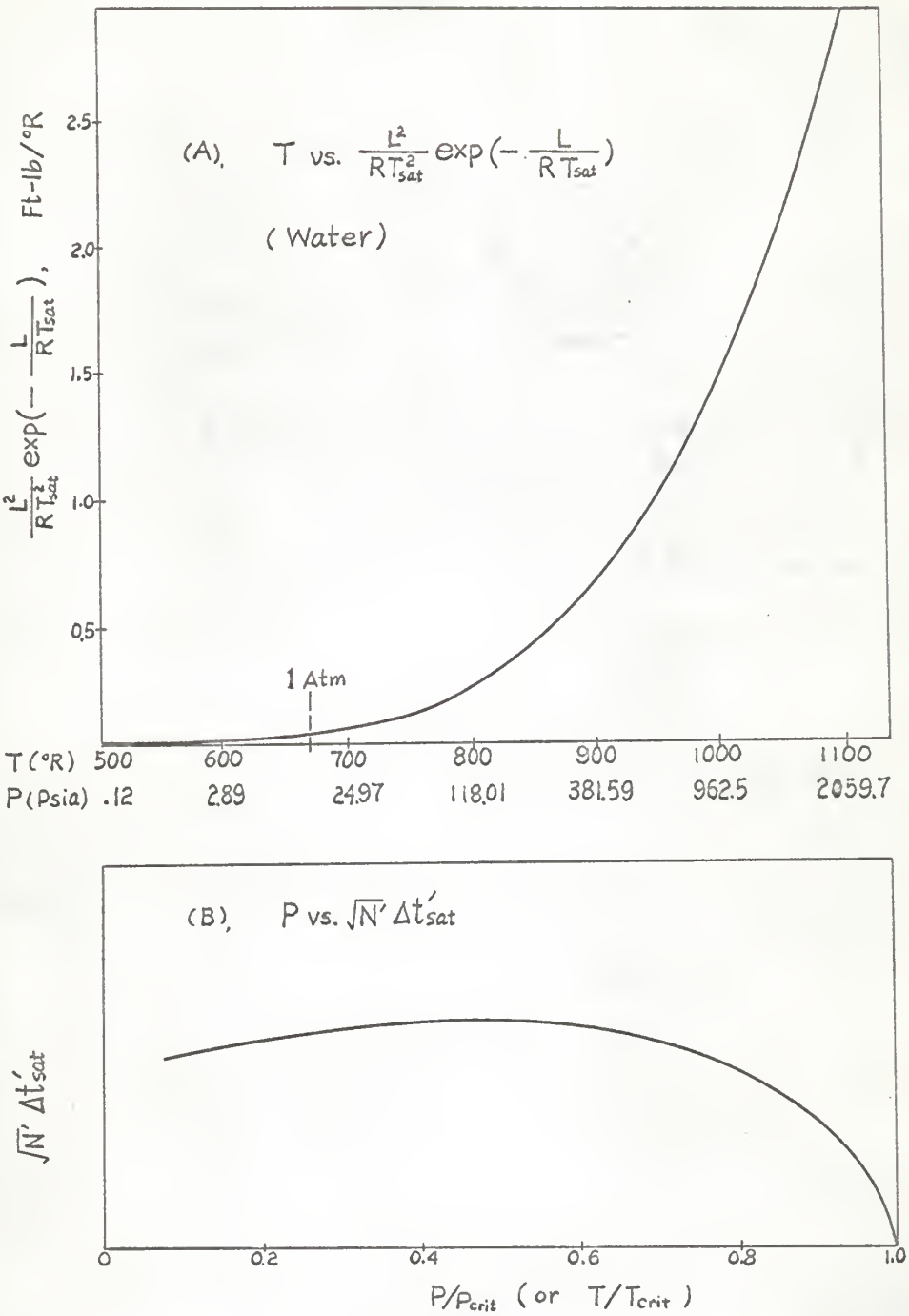

Fig. 22. Effect of temperature and pressure

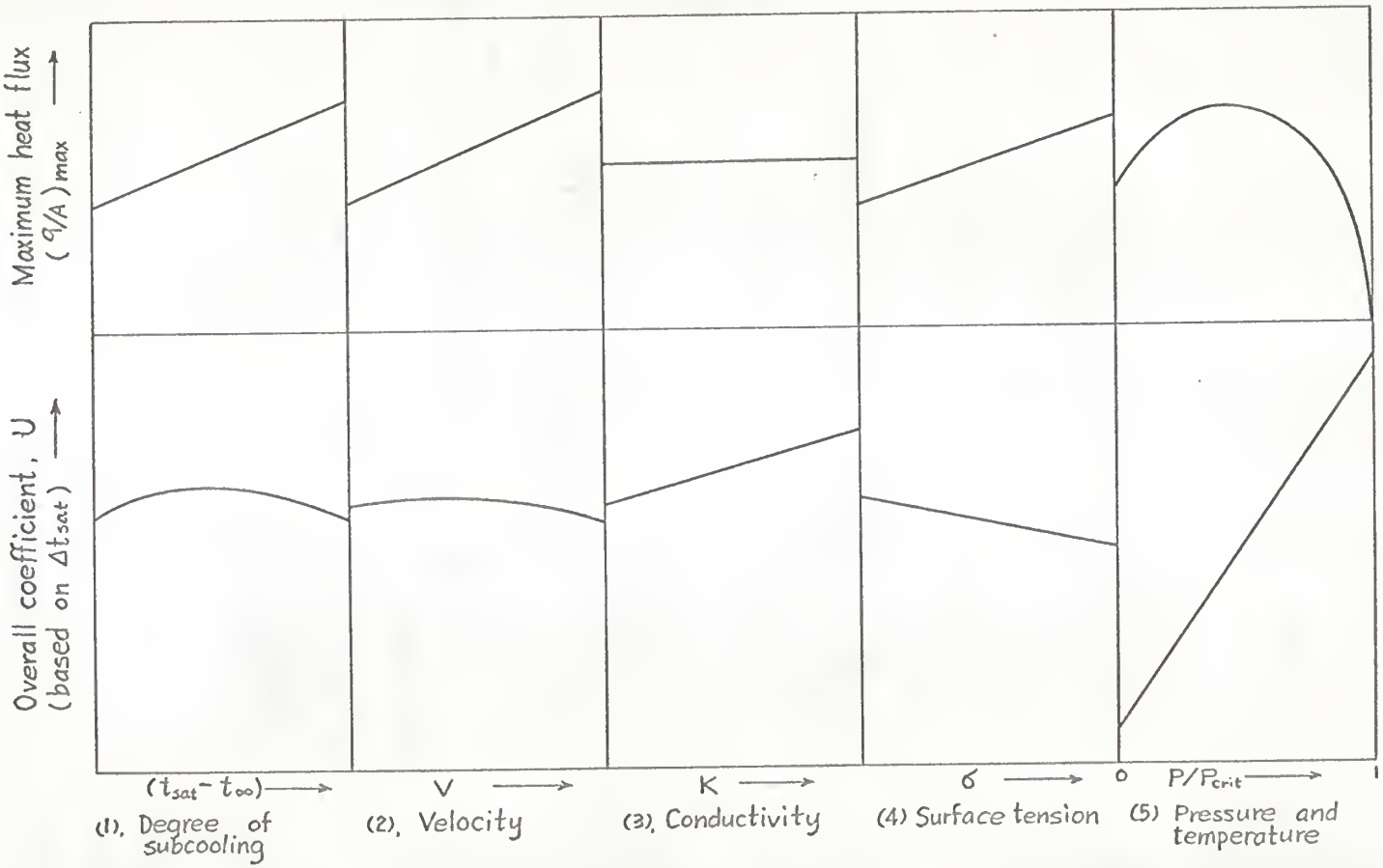

Fig.23. Factors affecting nucleate boiling heat transfer

it is clear that all the factors that affect nucleate boiling heat transfer are explained very well by the new triple interface evaporation mechanism.

3-5. Conclusion

Although many excellent works show that bubble stirring action dominates the heat transfer rate at low nucleate boiling ranges, there are facts which reveal that at a high nucleate boiling region, heat flux is mostly contributed by latent heat transport. The large amount of heat that is transported passes through the bubble via a very small area near the solid-liquid-vapor triple interface at the bubble base. The heat flux is entirely determined by the superheat, Δt_{sat} and the total bubble circumferences that are in contact with the heating surface. Prediction of heat flux under any circumstance will be possible if the relation between bubble population, bubble diameter and superheat is clear.

From an available relation observed by Gaertner and Westwater (33), the triple interface evaporation mechanism shows that the heat flux is proportional to $N^{0.401}$ in the high flux range and varies directly with N in the low flux range. Both results agree with the experiments of Gaertner, Westwater, and Jakob.

As the most unexplainable factors in most proposed mechanisms, subcooling and velocity are shown in the new

mechanism to give no more heat flux at a given superheat Δt_{sat}, while they do increase the peak flux to a certain extent. As a preliminary treatment, a single equation which successfully explains all the factors, subcooling, velocity, thermal conductivity, surface tension and pressure that affect the necleate boiling heat transfer has been derived by the author of this report.

ACKNOWLEDGMENT

The writer sincerely thanks Dr. N. Z. Azer and Dr. Ralph G. Nevins for their invaluable advice in writing this report and Dr. C. L. Hwang and Dr. L. T. Fan for their help in literature survey.

An acknowledgment is also made to Dr. W. Tripp whose lectures are always so instructive and that have constantly been a source of inspiration.

NOMENCLATURE

A	=	area of heat transmission, ft^2
a	=	evaporation constant defined in Eq. (13), lb/hr ft
b	=	constant defined in Eq. (17), ft^2/hr
d	=	instantaneous bubble diameter, ft
d_c	=	instantaneous bubble contact diameter, ft
d_o	=	detaching bubble diameter, ft
d'_o	=	detaching bubble diameter at critical heat flux, ft
d^*	=	mean effective bubble diameter defined in Eq. (19), ft
K	=	thermal conductivity, BTU/hr ft deg F
k	=	Boltzmann gas constant, BTU/molecule deg F
L	=	latent heat of vaporization, BTU/lb
$\dot{m}$	=	mass rate of evaporation, lb/hr ft^2
N	=	bubble population, Bubbles/ft^2
N'	=	bubble population at peak heat flux, bubbles/ft^2
P	=	pressure, lb/ft^2
P_v	=	vapor phase pressure, lb/ft^2
q	=	heat rate, BTU/hr
R	=	gas constant, BTU/lb deg F
R	=	bubble radius, ft
r	=	bubble radius, ft
T	=	absolute temperature, deg R
T_{sat}	=	absolute saturation temperature, deg R

T_w = absolute wall temperature, deg R

T_∞ = absolute bulk temperature, deg R

V = volume, ft^3

β = contact angle, deg

δ = effective thickness defined in Eq. (12), ft

σ = surface tension, lb/ft

ρ = density, lb/ft^3

ρ_v = density of vapor, lb/ft^3

ρ_L = density of liquid, lb/ft^3

Δt = temperature difference, deg F

Δt_{sat} = $t_w - t_{sat}$, deg F

$\Delta t'_{sat}$ = degree of superheat at peak flux, deg F

θ = time, hr

γ = constant defined in Eq. (22)

N_{NU} = bubble Nusselt number, dimensionless

N_{RE} = Reynold number, dimensionless

N_{PR} = Prandtl number, dimensionless

$(q/A)_{LH}$ = heat flux due to latent heat transport, BTU/hr ft^2

$(q/A)_{TOT}$ = total heat flux, BTU/hr ft^2

REFERENCES

1. Jakob, M., Heat Transfer, Vol. 1, John Wiley & Sons (1949).

2. McAdams, W. H., Heat Transmission, 3rd Ed., McGraw-Hill, New York (1954).

3. Rohsenow, W. M., "Heat Transfer with Boiling," in Developments in Heat Transfer, edited by W. M. Rohsenow, MIT Press, (1964).

4. Westwater, J. W., "Boiling of Liquid," in Advances in Chemical Engineering, Vol. 1 (1956) and Vol. 2 (1958), edited by T. B. Drew and J. W. Hooper, Academic Press, New York.

5. Leppert, G. and C. C. Pitts, "Boiling," in Advances in Heat Transfer, edited by T. F. Irvine, Jr. and J. H. Hartnett, Academic Press (1964).

6. Tong, L. S., Boiling Heat Transfer and Two-Phase Flow, Wiley & Sons, New York (1964).

7. Nukiyama, S., "Maximum and Minimum Values of Heat Transmitted from Metal to Boiling Water Under Atmospheric Pressure," J. of Soc. Mech. Engrs., Japan 37, p. 376 (1934). Cited in Ref. (6).

8. Cryder, D. S. and E. R. Gilliland, "Heat Transmission from Metal Surfaces to Boiling Liquids," Ind. Eng. Chem. 24, p. 1382 (1932).

9. Cryder, D. S. and A. C. Finalbargo, "Heat Transmission from Metal Surfaces to Boiling Liquids: Effect of Temperature of the Liquid on Film Coefficient," Trans. A.I.Ch.E. 33, p. 346 (1937).

10. Jakob, M., and W. Linke, "Heat Transmission in the Evaporation of Liquids at Vertical and Horizontal Surfaces," Z. Physik 36, p. 267 (1935). Cited in Ref. (1).

11. Insinger, T. H. and H. Bliss, "Transmission of Heat to Boiling Liquids," Trans. A.I.Ch.E. 36, p. 491 (1940).

12. Bonilla, C. F. and C. W. Perry, "Heat Transmission to Boiling Binary Liquid Mixtures," Trans. A.I.Ch.E. 37, p. 685 (1941).

13. Rohsenow, W. M., "A Method of Correlating Heat Transfer Data for Surface Boiling of Liquids," Trans. ASME 74, p. 969 (1952).

14. Forster, H. K. and N. Zuber, "Dynamics of Vapor Bubbles and Boiling Heat Transfer," A.I.Ch.E. J. 1, p. 531 (1955).

15. Rohsenow, W. M. and J. A. Clark, "A Study of the Mechanism of Boiling Heat Transfer," Trans. ASME 73, p. 609 (1951).

16. Gunther, F. C. and F. Kreith, "Photo Graphic Study of Bubble Formation in Heat Transfer to Subcooled Water," Jet Propulsion Laboratory Progress Report 4-120, C.I.T. (1950). Cited in Ref. (6).

17. Gilmour, C. H., "Nucleate Boiling - a Correlation," Chem. Eng. Progr. 54, p. 77 (1958).

18. Kutateadz, S. S., "Heat Transfer During Condensation and Boiling," (Mashgiz, Moscow, 1949, 1952), Atomic Energy Commission Translation 3770, Tech. Info. Service, Oak Ridge, Tenn. Cited in Ref. (23).

19. Yamagata, K. and K. Nishikawa, "On the Correlation of Nucleate Boiling Heat Transfer," Int. J. Heat Mass Transfer 1, p. 219 (1960).

20. Zuber, N., "Nucleate Boiling, the Region of Isolated Bubbles and the Similarity with Natural Convection," Int. J. Heat Mass Transfer, 5, p. 53 (1963).

21. Tien, C. L., "A Hydrodynamic Model of Nucleate Pool Boiling," Int. J. Heat Mass Transfer 5, p. 533 (1962).

22. Sato, "A Review in Boiling and Condensation," Chem. Eng. Japan 27, No. 3, p. 187 (1963).

23. Zuber, N. and E. Fried, "Two-Phase Flow and Boiling Heat Transfer to Cryogenic Liquids," Amer. Rocket Soc. J. 32, No. 9, p. 1332 (1962).

24. Moore, F. D. and R. B. Mesler, "The Measurement of Rapid Surface Temperature Fluctuations During Nucleate Boiling of Water," A.I.Ch.E. J. 7, p. 620 (1961).

25. Bankoff, S. G. and J. P. Mason, "Heat Transfer from the Surface of a Steam Bubble in Turbulent Subcooled Liquid Stream," A.I.Ch.E. J. 8, p. 30 (1962).

26. Bankoff, S. G., "A Note on Latent Heat Transport in Nucleate Boiling," A.I.Ch.E. J. 8, p. 60 (1962).

27. Rogers, T. F. and R. B. Mesler, "An Experimental Study of Surface Cooling by Bubbles During Nucleate Boiling of Water," A.I.Ch.E. J. 10, p. 656 (1964).

28. Rallis, C. J. and H. H. Jawurek, "Latent Heat Transport in Saturated Nucleate Boiling," Int. J. Heat Mass Transfer 7, p. 1051 (1964).

29. Westwater, J. W. and J. G. Santangelo, "Photographic Study of Boiling," Ind. Eng. Chem. 47, p. 1605 (1955).

30. Johnson, Jr., M. A., Javier de la Pena and R. B. Mesler, "Bubble Shapes in Nucleate Boiling," Chem. Eng. Progr. Symp. Ser. No. 64, Vol. 62, p. 1 (1966).

31. Bankoff, S. G., "On the Mechanism of Subcooled Nucleate Boiling," Chem. Eng. Progr., Symp. Ser. No. 32, P. 157 (1961).

32. Gibbs, W., Collected Work, Vol. 1, p. 229, Dover, (1961).

33. Hsu, Y. Y. and R. W. Graham, "An Analytical and Experimental Study of the Thermal Boundary Layer and Ebillition Cycle in Nucleate Boiling," NASA-TN-D-594 (1961).

34. Clark, H. B., P. H. Strenge, and J. W. Westwater, "Active Sites for Nucleate Boiling," Chem. Eng. Progr. Symp. Ser. No. 29, Vol. 55, p. 103 (1959).

35. Griffith, P. and J. D. Walls, "The Role of Surface Conditions in Nucleate Boiling," Chem. Eng. Prog., Symp. Ser. No. 30, p. 49 (1960).

36. Keenan, J. H., Thermodynamics, p. 437, John Wiley & Sons, New York (1941).

37. Lord Rayleigh, O. M., "Pressure Due to Collapse of Bubbles," Phil. Mag. 34, p. 94 (1917).

38. Forster, H. K. and N. Zuber, "Growth of a Vapor Bubble in a Superheated Liquid," J. Appl. Phys. 25, p. 474 (1954).

39. Plesset, M. S. and S. A. Zwick, "The Growth of Vapor Bubbles in Superheated Liquids," J. Appl. Phys. 25, p. 493 (1954).

40. Cited in Ref. (2).

41. Forster, K. E. and R. Greif, "Heat Transfer to Boiling Liquid, Mechanism and Correlations," Trans. ASME, Ser. C. J. Heat Transfer 81, p. 43 (1959).

42. Lyon, R. E., A. S. Foust and D. L. Katz, "Boiling Heat Transfer with Liquid Metals," Chem. Eng. Progr., Symp. Ser. No. 7, p. 41 (1955).

43. International Critical Table, 1st ed., Vol. 3, p. 237, McGraw-Hill, New York (1929).

44. Combustion, J., Vol. 25, No. 7 p. 38 (1954).

45. Griffith, P., "Bubble Growth Rates in Boiling," Trans. ASME 80, p. 721 (1958).

46. Alty, T., "The Maximum Rate of Evaporation of Water," Phil. Mag. 15, p. 82 (1933).

47. Soo, S. L., Analytical Thermodynamics, p. 93, Prentice-Hall, New York (1962).

48. Carslaw, H. S. and J. C. Jaeger, Conduction of Heat in Solid, p. 166, 2nd ed., Oxford (1959).

49. Costello, C. P. and E. R. Redeker, "Boiling Heat Transfer and Maximum Heat Flux for a Surface with Coolant Supplied by Capillary Wicking," Chem. Eng. Prog., Symp. Ser. No. 41 (1963).

50. Westwater, J. W., "Boiling of Liquids," Amer. Scientist, Vol. 47, p. 427 (1959).

51. Gaertner, R. F. and J. W. Westwater, "Population of Active Sites in Nucleate Boiling Heat Transfer," Chem. Eng. Prog., Symp. Ser. No. 30, p. 39 (1960).

52. Jakob, M., "Local Temperature Differences as Occurring in Evaporation, Condensation, and Catalytic Reaction," in Temperature, Its Measurement and Control in Science and Industry, p. 834, Reinhold, New York, Vol. 1. (1941).

APPENDIX 1

APPENDIX 1. CONVERGENCE OF EQUATION (10).

The series,

$$\left.\frac{\partial t}{\partial x}\right|_{x=o} = \frac{4(t_w - t_{sat})}{a} \sum_{o}^{\infty} \text{Sinh}\frac{(a-y)(2n+1)\pi}{a}\,\text{Cosech}\,(2n+1)\pi \qquad (10)$$

becomes infinite when y = 0. Since at y = 0,

$$\left.\frac{\partial t}{\partial x}\right|_{x=o,\,y=o} = \frac{4(t_w - t_{sat})}{a} \sum_{o}^{\infty} 1 = \infty$$

But for any $y > 0$ ($y \neq 0$), the series can be written,

$$\left.\frac{\partial t}{\partial x}\right|_{x=o} = \frac{4(t_w - t_{sat})}{a} \sum_{o}^{\infty} \frac{e^{\frac{(a-y)(2n+1)\pi}{a}} - e^{-\frac{(a-y)(2n+1)\pi}{a}}}{2} \cdot \frac{2}{e^{(2n+1)\pi} - e^{-(2n+1)\pi}}$$

$$< \frac{4(t_w - t_{sat})}{a} \sum_{o}^{\infty} \frac{e^{(2n+1)\pi}\, e^{-\frac{y}{a}(2n+1)\pi}}{e^{(2n+1)\pi} - e^{-(2n+1)\pi}}$$

or

$$\frac{a}{4(t_w - t_{sat})} \left.\frac{\partial t}{\partial x}\right|_{x=o} < \sum_{o}^{\infty} \frac{e^{-\frac{y}{a}(2n+1)\pi}}{1 - e^{-(4n+2)\pi}}$$

$$< \sum_{o}^{\infty} \frac{e^{-\frac{y}{a}(2n+1)\pi}}{1 - e^{-2\pi}}$$

$$< \frac{1}{1 - e^{-2\pi}} \sum_{o}^{\infty} e^{-\frac{y}{a}(2n+1)\pi}$$

$$< \frac{1}{1 - e^{-2\pi}} \sum_{o}^{\infty} e^{-\frac{y}{a}2n\pi}$$

Since $\sum_{0}^{\infty} e^{-\frac{y}{a}2n\pi}$ is a geometric series with common ratio $e^{-\frac{2y\pi}{a}}$ for any $y=\delta$, $\delta>0$

$$e^{-\frac{2y\pi}{a}} = \frac{1}{e^{\frac{2\pi y}{a}}} < 1$$

Moreover,

$$\left| e^{-\frac{y}{a}2n\pi} \right| \leq \left| e^{-\frac{\delta}{a}2n\pi} \right|$$

for all y with $\delta \leq y \leq a$, $\delta > 0$. Since $\sum_{0}^{\infty} e^{-\frac{\delta}{a}2n\pi}$ converges from the Weierstrass Comparation Test, it is known that Eq. (10) converges uniformly in the interval $\delta \leq y \leq a$, $\delta > 0$.

APPENDIX 2

APPENDIX 2. NUMERICAL VALUATION OF $Q_{\delta-a}$ FROM EQ. (11).

Equation (11) is written,

$$Q_{\delta-a} = -\frac{4K(t_w - t_{sat})}{\pi} \sum_{0}^{\infty} \frac{1}{(2n+1)} \left[1 - \operatorname{Cosh} \frac{(a-\delta)(2n+1)\pi}{a}\right] \operatorname{Cosech}(2n+1)\pi \qquad (11)$$

Let $a-\delta = ma$, i.e. $m = 1 - \frac{\delta}{a}$, where $0 \leq m < 1$. Then,

$$\left[1 - \operatorname{Cosh} \frac{(a-\delta)(2n+1)\pi}{a}\right] \operatorname{Cosech}(2n+1)\pi$$

$$= \left[1 - \operatorname{Cosh} m(2n+1)\pi\right] \operatorname{Cosech}(2n+1)\pi$$

$$= \left[1 - \frac{e^{m(2n+1)\pi} + e^{-m(2n+1)\pi}}{2}\right] \frac{2}{e^{(2n+1)\pi} - e^{-(2n+1)\pi}}$$

$$= \left[-\frac{e^{m(2n+1)\pi} - 2 + e^{-m(2n+1)\pi}}{e^{(2n+1)\pi} - e^{-(2n+1)\pi}}\right]$$

$$= -\frac{\left[e^{\frac{m}{2}(2n+1)\pi} - e^{-\frac{m}{2}(2n+1)\pi}\right]^2}{e^{(2n+1)\pi} - e^{-(2n+1)\pi}} \qquad (A)$$

For $m \geq 0.5$, the terms $e^{-\frac{m}{2}(2n+1)\pi}$ and $e^{-(2n+1)\pi}$ can be neglected for all n except n=0. This can be justified by calculating the maximum error that resulted from this neglect, when n=1, m=0.5 as,

$$\epsilon = \frac{\frac{\left[e^{0.75\pi} - e^{-0.75\pi}\right]^2}{e^{3\pi} - e^{-3\pi}} - \frac{e^{1.5\pi}}{e^{3\pi}}}{\frac{\left[e^{0.75\pi} - e^{-0.75\pi}\right]^2}{e^{3\pi} - e^{-3\pi}}}$$

$$\epsilon = \frac{0.00934 - 0.00905}{0.00934} = 3.11\,\%$$

For higher n and m, the error will be greatly reduced; thus this action is reasonable. Equation (A) becomes,

$$\left[1-\cosh\frac{(a-\delta)(2n+1)\pi}{a}\right]\operatorname{cosech}(2n+1)\pi = -\frac{e^{m(2n+1)\pi}}{e^{(2n+1)\pi}} = -e^{(m-1)(2n+1)\pi}$$

where n = 1, 2, 3,..., $m \geq 0.5$ Substituting the above result into Eq. (11), results in

$$Q_{\delta-a} = \frac{4K(t_\omega - t_{sat})}{\pi}\left[\frac{(e^{\frac{m}{2}\pi} - e^{-\frac{m}{2}\pi})^2}{e^{\pi} - e^{-\pi}} + \sum_{n=1}^{\infty}\frac{1}{(2n+1)}\, e^{(m-1)(2n+1)\pi}\right]$$

Since

$$\sum_{n=0}^{\infty}\frac{1}{(2n+1)}\chi^{(2n+1)} = \frac{1}{2}\ln\left(\frac{1+\chi}{1-\chi}\right)$$

Putting $e^{(m-1)\pi} = \chi$, gives

$$Q_{\delta-a} = \frac{4K(t_\omega - t_{sat})}{\pi}\left[\frac{(e^{\frac{m}{2}\pi} - e^{-\frac{m}{2}\pi})^2}{e^{\pi} - e^{-\pi}} - e^{(m-1)\pi} + \frac{1}{2}\ln\left(\frac{1+e^{(m-1)\pi}}{1-e^{(m-1)\pi}}\right)\right].$$

The value of $\frac{\pi Q_{\delta-a}}{4K(t_\omega - t_{sat})}$ for various m is tabulated as follows:

m	$\frac{\delta}{a}$	$\frac{\pi Q_{\delta-a}}{4K(t_\omega - t_{sat})}$
0.0	1.0	0.000
0.5	0.5	0.135
0.7	0.3	0.332
0.9	0.1	0.845
0.95	0.05	1.172
0.99	0.01	1.844

APPENDIX 3

APPENDIX 3. EFFECTIVE THICKNESS OF WATER.

In Section 3-2 it is shown that for water at peak heat flux, the total heat transfer area is 20% of the heating surface area. Thus for a semi-spherical bubble, Eq. (26) gives a heat transfer area per unit heating surface area as

$$\pi d_o' N' \delta = \pi \delta d_o' \times 1.15 \left(\frac{9}{4} \cdot \frac{1}{d_o'^2}\right) = 8.15 \delta \frac{1}{d_o'}$$

Since this area should equal 0.2, that is

$$8.15 \delta = 0.2 d_o'$$

or

$$\delta = \frac{d_o'}{40.75}$$

which shows the effective thickness is really very small.

NUCLEATE BOILING HEAT TRANSFER

by

LIANG-CHUAN PENG
Diploma, Taipei Institute of Technology, 1960

AN ABSTRACT OF A MASTER'S REPORT

submitted in partial fulfillment of the

requirements for the degree

MASTER OF SCIENCE

Department of Mechanical Engineering

KANSAS STATE UNIVERSITY
Manhattan, Kansas

1966

ABSTRACT

Since 1960, the latent heat transport in nucleate boiling heat transfer has received considerable study and its contribution has been revised. Recently it has been observed by several investigators that latent heat transport is significant at all stages of nucleate boiling. The purpose of this report is to further verify the contribution of latent heat transport and to give a theoretical analysis of this mechanism.

The data of Westwater and Santangelo show that the latent heat transport contributes about 50% of the total heat flux observed in boiling saturated liquid at moderate heat flux range. Careful examination reveals that the heat flow into the bubble from heating surface passes through a very narrow area near the solid-liquid-vapor triple interface. A triple interface evaporation mechanism is thus proposed on the basis of this investigation. The equation of bubble growth rate derived by this mechanism has the form

$$R = \text{Const} \sqrt{\theta \tan \frac{\beta}{2}}$$

This agrees with the recent observation made by Johnson, Jr. and coworkers. The correlation of heat flux contributed by latent heat transport as derived by the author of this report is

$$q/A = \text{Const } N\, d_o \frac{L^2}{RT_{sat}^2} \exp\left(\frac{L}{RT_{sat}}\right) \Delta t_{sat}$$

This equation has been used successfully to explain the mechanism by which the factors pressure, velocity, degrees of subcooling, surface tension, and thermal conductivity of the heating surface affect nucleate boiling.